

**CORROSIVE WEAR BEHAVIOR OF ZIRCONIUM IN HOT SULFIDE
CONTAINING ELECTROLYTES**

Derrill Rodger Holmes

B.S. Oregon State University, Corvallis, Oregon 1976

A thesis presented to the faculty of the
Oregon Graduate Institute of Science and Technology
in partial fulfillment of the requirements for the degree
Masters of Science
in
Materials Science and Engineering

February 2001

The dissertation "Corrosive Wear Behavior of Zirconium in Hot Sulfide containing Electrolytes" by Derrill R. Holmes has been examined and approved by the following Examination Committee.

Dr. David Atteridge, Thesis Advisor ✓
Professor
Department of Materials Science and Engineering
Oregon Graduate Institute of Science and Technology

Dr. Margaret Ziomek-Moroz 0
Research Chemist
U.S. Department of Energy
Albany Research Center

Dr. Jack Devletian, Professor
Department of Materials Science and Engineering
Oregon Graduate Institute of Science and Technology

Dr. Te-Lin Yau, Metallurgist and Corrosion Engineer
Te-Lin Yau Consultancy
Albany, Oregon

Mr. Jack Tosdale, Senior Corrosion Engineer
Wah Chang
Albany, Oregon

Acknowledgments

I would like to thank Wah Chang, Albany for supporting this research and my education in general. I would also like to thank the Department of Energy, Albany Research Center for the use of their facilities. Specifically I would like to thank Dr. Jeffery Hawk, Mr. Joe Tylczak for the use of his equipment and his advice, and Dr. Margaret Ziomek-Moroz for her tireless effort and her support in preparation of this thesis. My thesis committee also deserves my thanks for their time and advice. Dr. Te-Lin Yau deserves my special thanks for piquing my interest in corrosion studies. And finally, I would like to thank my wife Ruth for doing double duty on many occasions and my boys James and William for understanding why I could not always be with them at their various activities.

Table of Contents

Acknowledgments	iii
Table of Contents	iv
List of Tables	vii
List of Figures	viii
Abstract	x
Chapter 1. Introduction	1
1.1 General description of Zirconium and Zirconium alloys	3
1.1.1 Occurrence and Applications	5
1.1.2 Use in the Nuclear Power Generation Industry	7
1.1.3 Use in the Chemical Producing Industry	8
1.2 Chemical and Physical properties of Zirconium	9
1.2.1 Chemical properties of Zirconium.....	9
1.2.2 Physical properties of Zirconium	15
1.3 Corrosion behavior of Zirconium	19
1.3.1 Acidic solutions	19
1.3.2 Neutral solutions	23
1.3.3 Alkaline solutions	23
1.3.4 Aqueous Organic solutions	23
1.3.5 Kraft solutions	24
1.3.6 Molten salts	26

1.4	Wear behavior of Zirconium	27
1.5	Overview of Pulping Processes	30
1.5.1	Kraft Process	30
1.5.2	Other pulping processes	34
Chapter 2.	Research Objectives	36
Chapter 3.	Experimental Methods	37
3.1	Materials	
3.1.1	Electrochemical Specimens	44
3.1.2	Wear Specimens	44
3.1.3	Electrolyte	46
Chapter 4.	Results and Discussion	48
4.1	Experimental Results	
4.1.1	Potentiodynamic Polarization Experiments	48
4.1.2	Polarization Resistance Experiments	54
4.1.3	Open Circuit Potential Experiments	59
4.1.4	Wear Experiments.....	61
4.1.5	Corrosive Wear Experiments.....	71
4.2	Determination of corrosive wear synergism	81
Chapter 5.	Conclusions	83
Chapter 6.	Future Work	85

Chapter 7. Bibliography.....	86
Biographical Sketch	90

List of Tables

Table 1	Areas of Concern in the Pulp and Paper Industry	1
Table 2	Chemical Composition of Reactor Grades of Zirconium	3
Table 3	Chemical Composition of Commercial Grades of Zirconium	4
Table 4	EMF Series	10
Table 5	Galvanic Series in Seawater	11
Table 6	Atomic and Crystallographic Properties of Zr 702 and Zr 705 ...	16
Table 7	Thermal Properties of Zr 702 and Zr 705	17
Table 8	Mechanical Properties of Zirconium Alloys	18
Table 9	Typical Composition of Kraft Liquors	24
Table 10	Results of Slow Strain-Rate Tests	25
Table 11	Results of U-Bend Tests of Zirconium	26
Table 12	Hardness Profile of Zirconium with Enhanced Oxide Layer	29
Table 13	Composition of Specimens	45
Table 14	Initial Hardness of Specimens	45
Table 15	Chemical Composition of Typical Green Liquor	46
Table 16	Dissolved Metallic Ion Content of Green Liquor	47
Table 17	Summary of Polarization Resistance Data.	55
Table 18	Effect of Wear on Hardness	62
Table 19	Cumulative Volume Loss	82

List of Figures

Figure 1	Periodic Table	5
Figure 2	Influence of pH on Solubility.....	13
Figure 3	Potential - pH Diagram	14
Figure 4	Isocorrosion Diagram for Zirconium in Hydrochloric Acid	20
Figure 5	Isocorrosion Diagram for Zirconium in Nitric Acid	21
Figure 6	Isocorrosion Diagram for Zirconium in Sulfuric Acid	22
Figure 7	Recausticizing Circuit Diagram	33
Figure 8	Generalized Diagram of Electrochemical Setup	41
Figure 9	Diagram of Working Electrode	42
Figure 10	Generalized Diagram of Wear Apparatus	43
Figure 11	Anodic Polarization of Zirconium 702 with Pickled Surfaced in Green Liquor	50
Figure 12	Anodic Polarization of Zirconium 702 with Oxidized Surface in Green Liquor	51
Figure 13	Anodic Polarization of SS 304L in Green Liquor	52
Figure 14	Effect of Surface Treatment on Anodic Polarization	53
Figure 15	Polarization Resistance of Zirconium 702 with Pickled Surface in Green Liquor	56
Figure 16	Polarization Resistance of Zirconium 702 with Oxidized Surface in Green Liquor	57
Figure 17	Polarization Resistance of SS 304L in Green Liquor	58
Figure 18	Open Circuit Potential Comparison... ..	60
Figure 19	Volume Loss of Zirconium 702 with Pickled Surface in DI water... ..	63
Figure 20	Volume Loss of Zirconium 702 with Oxidized Surface in DI water ..	64
Figure 21	Volume Loss of SS 304L in DI water	65

Figure 22	Comparison of Volume Loss in DI water	66
Figure 23	Wear of Zirconium 702 with Pickled Surface in DI water.....	67
Figure 24	Wear of Zirconium 702 with Oxidized Surface in DI water	68
Figure 25	Wear of SS 304L in DI Water	69
Figure 26	Comparison of Wear Rate in DI water	70
Figure 27	Volume Loss of Zirconium 702 with Pickled Surface in Green Liquor	73
Figure 28	Volume Loss of Zirconium 702 with Oxidized Surface in Green Liquor	74
Figure 29	Volume loss of SS 304L in Green Liquor	75
Figure 30	Comparison of Volume Loss in Green Liquor	76
Figure 31	Wear Rate of Zirconium 702 with Pickled Surface in Green Liquor	77
Figure 32	Wear Rate of Zirconium 702 with Oxidized Surface in Green Liquor	78
Figure 33	Wear rate of SS 304L in Green Liquor	79
Figure 34	Comparison of Wear Rates in Green Liquor	80

Abstract

Corrosive Wear Behavior of Zirconium in Hot Sulfide Containing Electrolytes
Derrill Rodger Holmes, B.S.

M.S., Oregon Graduate Institute of Science and Technology
February 2001

Thesis Advisor: Dr. David Atteridge

The synergistic effect between corrosion and wear was determined for zirconium 702 in an aqueous medium. Zirconium 702 with a pickled surface treatment and zirconium 702 with an air oxidized surface treatment were studied. Stainless Steel 304L was used as a reference. The electrolyte used was actual Production Raw Green Liquor from the Pulp and Paper Industry. The testing conditions of 85°C and the chemical composition of the electrolyte are actual production conditions.

Electrochemical results showed that zirconium, in both the pickled and oxidized condition, had lower corrosion rates than the Stainless Steel 304L standard. Also, the electrochemical behavior of Zirconium 702 exhibited a less active surface than that of Stainless Steel 304L. Both the pickled surface and the oxidized surface exhibited this less active surface for zirconium 702.

The specimens with the oxidized surface had better wear characteristics when compared to the zirconium 702 with a pickled surface treatment. Both the volume loss and the wear rate showed that the zirconium 702 with the oxidized surface treatment was more wear resistant.

Synergism calculations showed that the zirconium 702 with the oxidized surface had the lowest interaction between pure wear and corrosive wear. Stainless Steel 304L had the highest interaction.

Chapter 1 Introduction

The Pulp and Paper Industry has always evolved in response to ever changing conditions. In recent times the emphasis has been placed on increasing yield, increasing quality and addressing environmental concerns. To address these concerns, the Materials Technology Institute of the Chemical Process Industries prepared the “Technology Roadmap”. [30] This roadmap provides a list of some of the major materials problems faced by the industry and gives major areas where new materials or technology is needed. These areas of concern are listed in Table 1.

Table 1
Areas of concern in the Pulp and Paper Industry.

1. Materials with high temperature/corrosion capabilities.
2. Materials for use in organic acids.
3. Materials for chlorine based processes.
4. Fluorine/halogens.
5. Lower cost materials for corrosive applications.
6. **Materials with wear resistance and liquid corrosion resistance.**
7. Heat exchange tubing with better corrosion resistance.
8. Materials that eliminate or resist stress corrosion cracking.
9. Reclamation/decontamination of process wastes.

Selection of material for high temperature/corrosion capabilities, material for chlorine based processes, fluorine/halogens, lower cost materials for corrosive applications and materials with wear resistance and liquid corrosion resistance are areas recognized to be of the highest priority. With the exception of the recommendation involving the use of chlorine and fluorides, zirconium could be a cost effective material for virtually all of the above requirements.

The corrosion resistance of zirconium in pulp and paper environments and organic acids has been well established by Yau.[15][21][26] Haygarth et.al. [8] [20] and Wehrenberg [23] have demonstrated zirconium's resistance to degradation under wear conditions. This coupled with zirconium's history of use in other chemical processing applications, in similar environments, should make zirconium a strong candidate for the material of choice in many areas of the Pulp and Paper Industry of the future.

However, the interaction of corrosion and wear needs to be determined for zirconium and its alloys. The area of interest and the subject of this thesis is the synergistic effect between corrosion and wear of zirconium and zirconium with an air oxidized surface. The electrolyte chosen for this study is green liquor obtained from a typical recausticizing circuit used in the Kraft pulping process.

1.1 General Description of Zirconium and Zirconium Alloys

Zirconium is a soft, grayish white, ductile and corrosion resistant metal. Zirconium alloys are divided into two alloy groups. One group is composed of those alloys used in nuclear applications. The second and larger group is those alloys used in non-nuclear applications.

The nuclear alloys are designed to give good corrosion resistance in high pressure and high temperature water and steam applications. These alloys are essentially hafnium free. They contain tin, iron, and chromium, or niobium as alloy additions. Table 2 gives the actual chemical composition of these alloys.

Table 2
Chemical Composition of
Nuclear Reactor Grade Zirconium Alloys
(Weight %)

	Hf	Sn	Nb	Fe	Cr	Ni	Fe+Cr	Fe+Cr +Ni
Zircaloy-2	.010	1.2-1.7	---	.07-.2	.05-.15	.03-.08	---	.18-.38
Zircaloy-4	.01	1.2-1.7	---	.18-.24	.07-.13	---	.28-.37	---
Zr-2.5Nb	.01	---	2.4-2.8	---	---	---	---	---

The non-nuclear alloys are generally low in alloy additions. In fact, the primary alloy for Chemical Processing Industry (CPI) use is commercially pure zirconium. This alloy is designed and processed to contain a minimum of impurities. This alloy group is used primarily in corrosion resistant applications for the CPI. Table 3 gives the chemical compositions of this group of alloys.

Table 3
 Chemical Composition of
 Commercial Grades of Zirconium
 (Weight %)

	Zr+Hf (min)	Hf (max)	Sn	Nb	Fe+Cr (max)	O
Zr 702 (UNS R60702)	99.1	4.5	---	---	.2	.16
Zr 704 (UNS R60704)	97.5	4.5	1.0-2.0	---	.2-.4	.18
Zr 705 (UNS R6-705)	95.5	4.5	---	2.0-3.0	.2	.18
Zr 706 (UNS R60706)	95.5	4.5	---	2.0-3.0	.2	.16

1.1.1 Occurrence and Applications of Zirconium

Zirconium is atomic number 40. This puts zirconium in group 4B of the periodic table along with titanium, and hafnium, see Figure 1.

d transition elements									
III A	IV A	V A	VI A	VII A	VIII A			I B	II B
21 2.99 Sc	22 4.51 Ti	23 6.09 V	24 7.19 Cr	25 7.47 Mn	26 7.87 Fe	27 8.8 Co	28 8.91 Ni	29 8.93 Cu	30 7.13 Zn
44.956	47.88	50.942	51.996	54.938	55.847	58.933	58.69	63.546	65.39
39 4.48 Y	40 6.51 Zr	41 8.58 Nb	42 10.22 Mo	43 11.50 Tc	44 12.36 Ru	45 12.42 Rh	46 12.00 Pd	47 10.5 Ag	48 8.65 Cd
88.906	91.224	92.906	95.94	(97.907)	101.07	102.906	106.42	107.87	112.41
57 6.17 La*	72 13.28 Hf	73 16.67 Ta	74 19.25 W	75 21.02 Re	76 22.58 Os	77 22.55 Ir	78 21.44 Pt	79 19.28 Au	80 - Hg
138.91	178.49	180.95	183.85	186.21	190.2	192.22	195.08	196.97	200.59
89 Ac**	104 Unq	105 Unp	106 Unh	----Atomic Number ----Density (g/cm ³) ----Element ---Atomic weight (amu)					
(227.03)	(261.11)	(262.11)	(262.12)						

d Transition Elements in the Periodic Table

Figure 1
Periodic Table

Zirconium has been considered a rare and exotic metal since its early isolation from ore in 1824. Actually, zirconium is the 18th most abundant element in the Earth's crust.[11] This makes it more plentiful than many metals, which are thought of as common materials of construction. Zirconium, for instance, is more abundant than nickel, copper, chromium, zinc, lead, or cobalt.[29]

The most important source of zirconium is zircon ($ZrO_2 \cdot SiO_2$). The usual source of the ore is placer deposits from ordinary beach sand where it concentrates along with other high density minerals such as rutile and ilmenite, both titanium ores, magnetite, an iron ore, and chromite, an important iron-chromium ore.[33][11]

With the exception of Antarctica, major commercial sources exist on all continents. Major producing countries include Australia, USA, South Africa, India, Sri Lanka, Madagascar, Norway, Brazil, and Ukraine.[11]

More than 800,000 metric tons of zirconium mineral concentrates were produced worldwide in 1998. Of this, greater than 95% was used for the production of zircon, zirconium oxide, and other zirconium chemicals. Zircon is the major form used in high temperature applications such as foundry molds, and refractory bricks used for lining molten metal crucibles. Yttria, magnesia, or calcia stabilized zirconium oxide (Zirconia) is used for high-strength structural ceramics, and coatings for high temperature turbine engine parts. Other uses of high purity zirconium chemicals include deodorant, paper treatment compounds, and paint formulations. The remaining 5% of zirconium concentrates produced in 1998 were used for metal and metal alloy production. The majority of the approximately 4,000 metric tons used for metal production went into standard forms used in the Chemical Processing Industry (CPI). Common forms include wire, rod, plate, sheet, foil, piping, tubing and a host of more specialized parts. Common uses are heat exchangers, piping and fittings, reaction columns, reaction vessels both lined and solid, pumps and pump parts formed from both cast and wrought material, agitators, and powder compact parts. The selection of typical zirconium forms and the use of fabricated structures by the CPI rely on the superior corrosion, wear, and corrosive-wear behavior of zirconium.

1.1.2 Use of Zirconium in the Nuclear Power Generation Industry

The main characteristics for materials of construction for the nuclear power generation industry are good high-temperature corrosion resistance, adequate strength, resistance to irradiation damage and transparency to thermal neutrons.[29] Zirconium meets all of these critical conditions. Two types of nuclear reactors are currently in use. These are the boiling water reactor (BWR) and the pressurized water reactor (PWR). Zirconium alloys are used in both types of reactors.

In pressurized water reactors, the nuclear fuel is used to heat water in the primary cooling loop. The heat is then transferred to the secondary cooling loop where it is used to spin a series of high and low pressure turbines to generate electricity. In the primary loop, the operating temperatures are up to 300°C and the pressure is held at a constant 2250 psi. This primary cooling loop is where the majority of zirconium is used. Zirconium used in the primary cooling loop is used for tubing containing fuel pellets, guide tubes, pressure tubes and related structural components.[29]

Zircaloy 2 (Zr-2) was the first nuclear grade zirconium produced. Since this initial development, Zircaloy 4 (Zr-4) has been developed in response to high hydrogen absorption rates in high-temperature conditions of the primary cooling loop. In Zr-4, the small amount of nickel in Zr-2 is replaced by iron. This small change gives better resistance to hydrogen absorption during service in high-temperature water conditions typical of pressurized water nuclear reactors.[29] The compositions of nuclear grade Zirconium alloys are given in Table 2.

The development of new chemical compositions is ongoing today perhaps even more so than in the early days of nuclear power plant design. Small changes in Zircaloy 2 and Zircaloy 4 compositions are being explored in virtually every part of the world where nuclear power is employed.

1.1.3 Use of Zirconium in the Chemical Processing Industry.

Zirconium has a long history of use in the Chemical Processing Industry. Zirconium plates, sheets, rods, pipes, tubes, castings, and all other common forms are commonly used in the manufacture of reaction columns, heat exchangers, pumps and other production equipment required in CPI applications.

Major chemical industries which use zirconium materials include the manufacture of acetic acid, nitric acid, sulfuric acid, ammonium nitrate fertilizer, semi-conductor production and the production of organic and specialty chemicals.

In the past zirconium, in many cases, was the material of last resort. In many highly corrosive production streams many of the more common materials of construction, such as Inconels, Hastelloys and Stainless Steels have been tried but found to be unserviceable. As a final consideration, zirconium was tried and in many cases performed well.

More and more, as new information and uses of zirconium are documented, zirconium is becoming the material of first choice for CPI applications. In many of the more severe or critical applications, zirconium is becoming the material of choice during the initial design stage. By identifying the most appropriate material of construction early many problems can be avoided. Table 3 gives the chemical composition of commercial grades of zirconium used in CPI applications.

In other cases, high purity of the product is the primary concern. Even slight corrosion rates of many materials will leave undesired metallic ions or unwanted coloration in the final product. In final products such as the ultra high purity chemicals used in the production of semiconductor devices, even small quantities of certain ions will render the semiconductor device defective. Zirconium with its lower corrosion rate and lack of many metallic alloying additions will reduce these undesired metallic ions. Because Zr^{+4} ions are colorless [10], they do not impart unwanted coloration on the final product. This is an important consideration during the production of photo electric sensitive products.

1.2 Chemical and Physical Properties of Zirconium

Zirconium used in the CPI industry is usually one of four available commercial alloys. These alloys are Zr 702, Zr 704, Zr 705, and Zr 706. Each alloy has specific mechanical, thermal and corrosion properties making each particular alloy uniquely suited for a specific application. Table 3 shows the chemical composition of these zirconium alloys.

Zr 702, or unalloyed zirconium, is by far the most commonly used zirconium alloy in CPI applications which require maximum corrosion resistance. Zr 702 also has the lowest strength of any of the four commercial alloys. All zirconium grades can be clad to higher strength materials such as mild steel or stainless steel. This allows their use in a wider range of applications which require higher strength.

1.2.1 Chemical Properties of Zirconium

This thesis will focus on Zr 702. As seen in Table 3, Zr 702 and other commercial grades may contain up to 4.5% hafnium. In this case, hafnium is not an alloy addition but rather a holdover from processing in which the hafnium content is not separated from the zirconium. The presence of hafnium in the alloy composition does not significantly affect the physical, mechanical, or corrosion properties.[29] Oxygen is controlled as an interstitial strengthening element. Lower oxygen grades are available (less than 1000 ppm oxygen) and are used in special applications requiring formability. Oxygen is also used in surface hardening. The addition of oxygen to the surface also has the effect of oxygen hardening even below the enhanced oxide layer.[8] The adherent protective oxide film on the surface of zirconium can form even at cryogenic temperatures and can protect the surface from chemical and mechanical attack up to 350°C.[29]

As seen in Table 4, zirconium is a highly reactive element. Its redox potential is -1.5V vs. the Saturated Hydrogen Electrode (SHE) at 25°C.[29] Chemically, zirconium is predominantly quadrivalent in its chemical combinations. The existence of oxides of zirconium other than valence of +4 is possible but unlikely.[10][37] This attribute, along with its strong affinity for oxygen, allows zirconium to form and repair its protective oxide film even in highly reducing environments such as hydrochloric acid and sulfuric acid up to approximately 70%. Its valence state of +4 renders its complexes and soluble ions colorless. This is of great advantage in some applications where color is of concern.

The protective oxide film is difficult to form or maintain in hydrofluoric acid, sulfuric acid above 70% and in oxidizing chloride solutions. The oxide film under these conditions cannot be reformed or maintained, subsequently zirconium is not normally useful in these environments.[29]

As seen in Table 4, titanium and aluminum are among the few metals with an active potential which is more negative than zirconium.

Table 4
EMF Series [35]

noble	$\text{Pt}^{2+} + 3\text{e}^-$	=	Pt	=	+1.118	V vs. SHE
	$\text{Cu}^{2+} + 2\text{e}^-$	=	Cu	=	+0.342	V vs. SHE
	$2\text{H}^+ + 2\text{e}^-$	=	H	=	0.000	V vs. SHE
	$\text{Ni}^{2+} + 2\text{e}^-$	=	Ni	=	-0.250	V vs. SHE
	$\text{Fe}^{2+} + 2\text{e}^-$	=	Fe	=	-0.440	V vs. SHE
	$\text{Zr}^{4+} + 4\text{e}^-$	=	Zr	=	-1.53	V vs. SHE
	$\text{Ti}^{2+} + 2\text{e}^-$	=	Ti	=	-1.62	V vs. SHE
	$\text{Al}^{3+} + 3\text{e}^-$	=	Al	=	-1.66	V vs. SHE
active						

Table 5 gives the position of Zirconium in the Galvanic Series in Seawater. Only Titanium, of the more common materials, has a more noble potential than Zirconium.

Table 5 [20]
Galvanic Series in Seawater

More Noble	Platinum
	Gold
	Titanium (passive)
	Silver
	Zirconium (passive)
	SS 316 (passive)
	SS 304 (passive)
	SS 410 (passive)
	Nickel
	Bronzes
	Copper
	Brasses
	Tin
	Lead
	SS 316 (active)
	SS 304 (active)
	Cast iron
	Steel or Iron
	Aluminum 2024
	Aluminum (commercially pure)
	Zinc
More Active	Magnesium and magnesium alloys

The following equations from the Pourbaix diagram for Zr-H₂O [10] illustrate the range of chemical reactions of zirconium in water, in acid solutions and in alkaline solutions. In all cases, the superior corrosion behavior of zirconium can be attributed to a protective oxide film. The oxide film may be monoclinic, tetragonal or cubic in crystalline structure depending upon the conditions under which the film forms.

Zirconium's chemical reaction in water is as follows.



The chemical reaction of zirconium in very acid solutions produces zirconic (Zr⁺⁴) and zirconyl (ZrO⁺⁺) ions. Zirconium's chemical reaction in very alkaline solutions produce zirconate ions (HZrO₃⁻).

In moderately acid, neutral and moderately alkaline solutions, zirconium could be able to form and maintain its oxide film.[10] From Figures 2 and 3, it would seem that zirconium has a tendency to corrode in very high pH and very low pH environments. From polarization resistant experiments, reported in chapter 4, this is obviously not the case. Pourbaix [10] explains this by pointing out the limited solubility of zirconate ions in alkaline solutions. The zirconate ions may form a protective film on zirconium in very high pH solutions. In very low pH solutions, Pourbaix attributes the low corrosion rate of zirconium to possible differences in the oxide layer actually formed on the surface of zirconium and the theoretical oxide whose data was used to generate the Potential-pH equilibrium diagrams. In addition, it is possible that alkaline zirconal ions may form on the surface of zirconium providing a passive layer.

The Potential - pH diagram (Figure 3) indicates that ZrO₂ may dissolve forming HZrO₃ in solutions where the pH is above 12-13 and at -0.6V (SHE). The pH of green liquor lies between 12 and 14. The corrosion potential of zirconium in green liquor at 85°C is approximately -0.359 V (SHE). This, according to Pourbaix, is on the threshold of dissolution of zirconium oxide to zirconate ions.

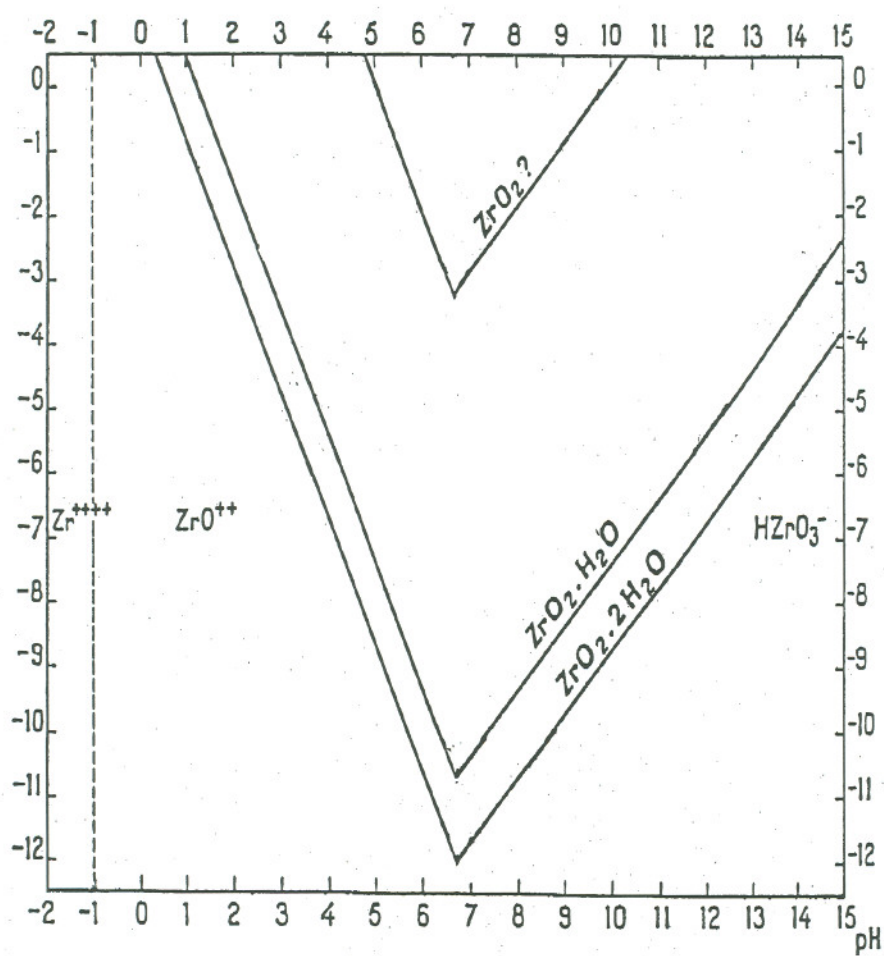


Figure 2 [10]
 Influence of pH on the solubility of ZrO_2 ,
 $ZrO_2 + H_2O$ and $ZrO_2 + 2H_2O$, at $25^\circ C$

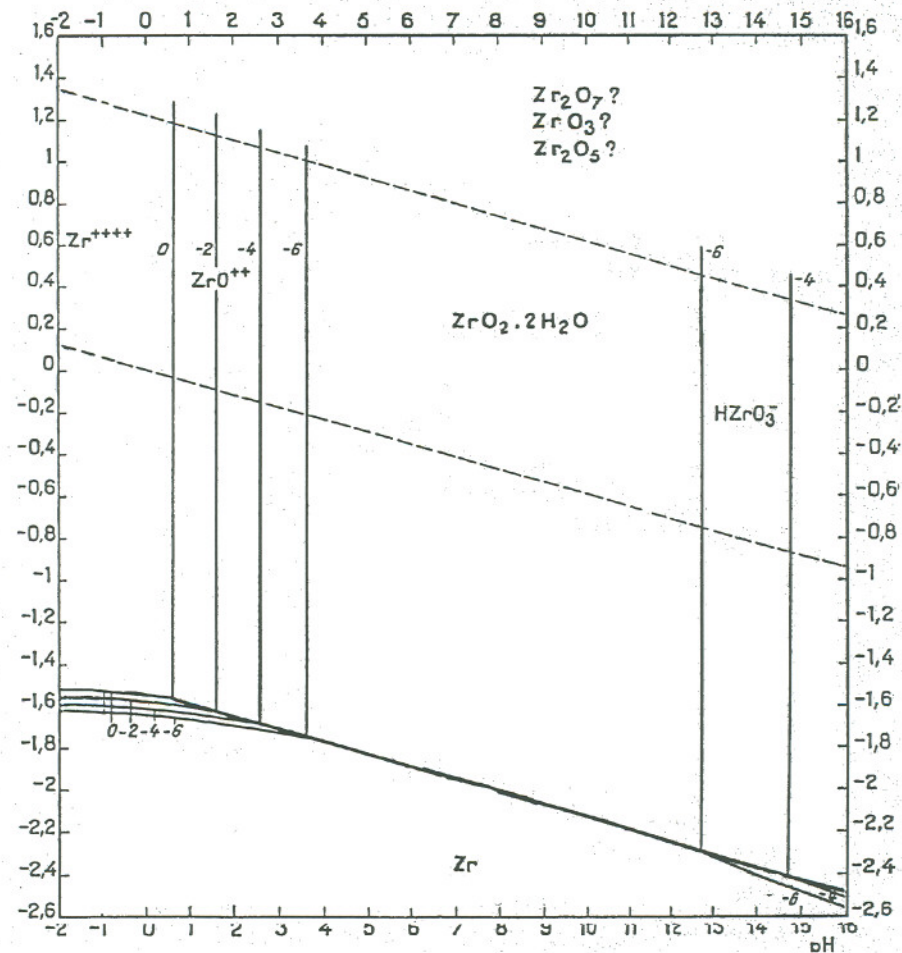


Figure 3 [10]
Potential - pH diagram for the System
Zirconium - Water at 25°C
pH vs. Potential (SHE)

1.2.2 Physical Properties of Zirconium

The atomic and crystallographic properties of Zr 702 and Zr 705 are outlined in Table 6. The thermal properties of Zr 702 and Zr 705 are listed in Table 7. The typical mechanical properties of all four commercial zirconium alloys are tabulated in Table 8.

Zirconium 702 is unalloyed zirconium, whereas Zirconium 704 is alloyed with Zr-Sn, Fe, and Cr. This alloy is used in applications requiring high corrosion resistance in high temperature and high pressure water and steam environments. This alloy is comparable to Zr 702 in corrosion resistance. Zirconium 705 (Zr-Nb alloy) has higher strength than Zr 702, but is slightly less corrosion resistant. The primary use is in applications calling for a higher degree of formability or higher strength with moderate corrosion resistance. Zirconium 706 (Zr-Nb alloy) has a lower oxygen content than Zr 705 and is more formable for applications such as plate heat exchangers.

As seen in Table 6, below 865°C (1590°F) zirconium exhibits hexagonal close packed crystal structure. This allows only one predominant slip plane system and three predominant twin systems. This structure accounts for the anisotropic characteristics of mechanical properties exhibited by zirconium. Some of the mechanical properties affected by this structure are thermal expansion, yield strength, ultimate tensile strength, elongation, notch toughness and bend ductility.

Table 6 [29]
Atomic and Crystallographic Properties
of Zr 702 and Zr 705

	702	705
Atomic Number	40	--
Atomic Weight	91.22	--
Atomic Radius		
Å (zero charge)	1.60-1.62	--
Å (+4 charge)	0.80-0.90	--
Density		
(g/cm ³ at 20°C)	6.510	6.640
(lb/in. ³)	0.235	0.240
Crystal structure		
α phase	Hexagonal close-packed (below 865°C)	No α phase below 865°C
β phase	Body-centered cubic (above 865°C)	Body-centered cubic (above 854°C)

Table 7 [29]
Thermal Properties of
Zr 702 and Zr 705

	Zr 702	Zr 705
Melting Point	1852°C (3365°F)	1840°C (3344°F)
Boiling Point	4377°C (7910°F)	4380°C (7916°F)
Coefficient of thermal expansion per °C		
25°C (72°F)	5.89 x 10 ⁻⁶	6.3 x 10 ⁻⁶
Thermal conductivity (300-800K)		
Btu-ft./h-ft ² -°F	13	10
W/m-K	22	17.1
Specific heat [Btu/lb/°F(32-212°F)]		
	0.068	0.067
Vapor pressure (mm Hg)		
2000°C (3632°F)	0.01	--
3600°C (6512°F)	900.0	---
Electrical resistivity [μ-cm at 20°C (68°F)]		
	39.7	55.0
Temperature coefficient of resistivity per °C		
20°C (68°F)	.0044	--
Latent heat of fusion (cal/g)	60.4	--
Latent heat of vaporization (cal/g)	1550	--

Table 8 [29]
Mechanical Properties of Zirconium Alloys
Room Temperature

	Minimum Tensile Strength (Mpa)	Minimum Yield strength (.2% offset), (Mpa)	Minimum Elongation % (0.2% Offset)	Bend Test Radius
Zr 702	380	207	16	5 T
Zr 704	414	240	14	5 T
Zr 705	552	380	16	3 T
Zr 706	510	345	20	2.5 T

1.3 Corrosion Behavior of Zirconium

The same thin autogenously formed and self healing oxide layer that gives zirconium its superior corrosion resistance in nuclear applications is also responsible for zirconium's superior corrosion resistance in a wide variety of industrial chemicals. Only a very few environments are able to break through this thin oxide layer and disrupt the self healing mechanism.[29] Among these are hydrofluoric acid, concentrated sulfuric acid, and oxidizing chloride solutions.

1.3.1 Acidic Solutions

Zirconium is resistant to attack in all mineral acids with the exception of hydrofluoric acid (HF).

Zirconium in halogen acids, again with the exception of hydrofluoric acid, exhibits very low corrosion rates in concentrated acids and at temperatures, in some cases, well above the boiling point. In 48% hydrobromic acid (HBr) zirconium has a corrosion rate of less than 0.125 mm/y (5 mpy). Hydriodic acid at a concentration of 57% and at temperatures of 250°C show a corrosion rates of less than 0.125 mm/y (5 mpy).[29]

The corrosion limits in hydrochloric acid, being one of the main uses for zirconium, is given as an isocorrosion curve in Figure 4. Limitations of the use in hydrochloric acid include the presence of oxidizing chloride ions such as ferric or cupric ions. Some of these limitations can be overcome by improving the surface condition. This can be accomplished by pickling in a hydrofluoric acid - nitric acid bath.[31][32] The pickling process removes surface contamination and smoothes the surface, reducing the tendency toward pitting in these environments.

A notable exception to the otherwise superior corrosion resistance of zirconium in halogen acids is hydrofluoric acid. Zirconium experiences rapid corrosion even in very low concentrations and temperatures in hydrofluoric acid solutions.

Along with the low corrosion rates in mineral acids, zirconium also shows relatively low tendency for stress corrosion cracking in these acids.[29]

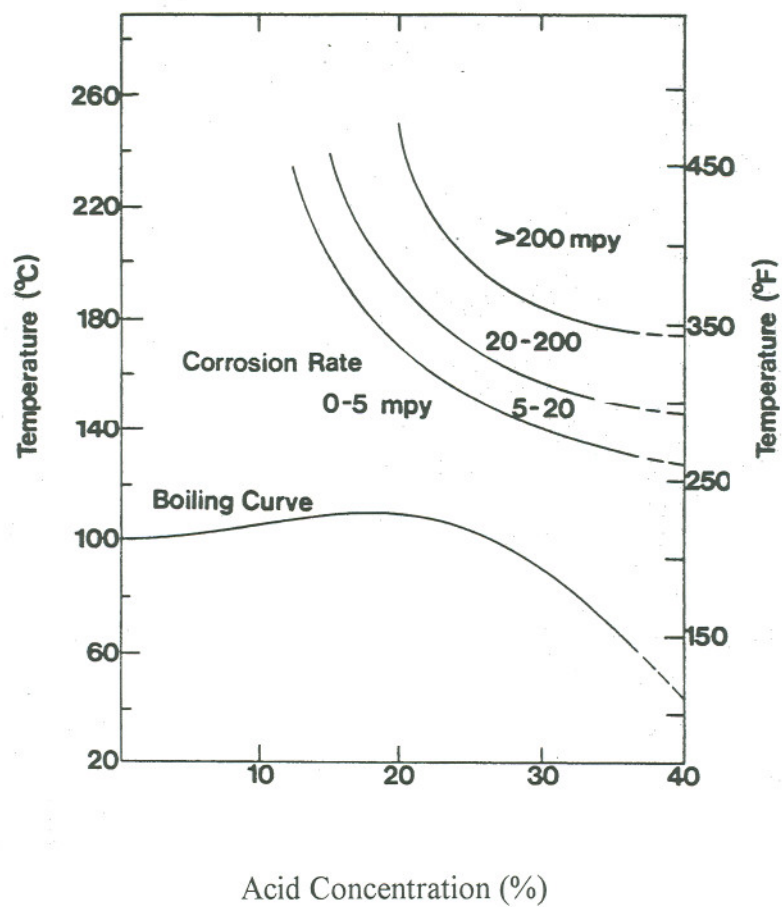


Figure 4
Isocorrosion curve for Zirconium 702 in Hydrochloric Acid

In nitric acid, zirconium experiences virtually no corrosion in acid concentrations of 98% at boiling temperature. In 70% acid zirconium sees service to 250°C (480°F), see Figure 5. [38]

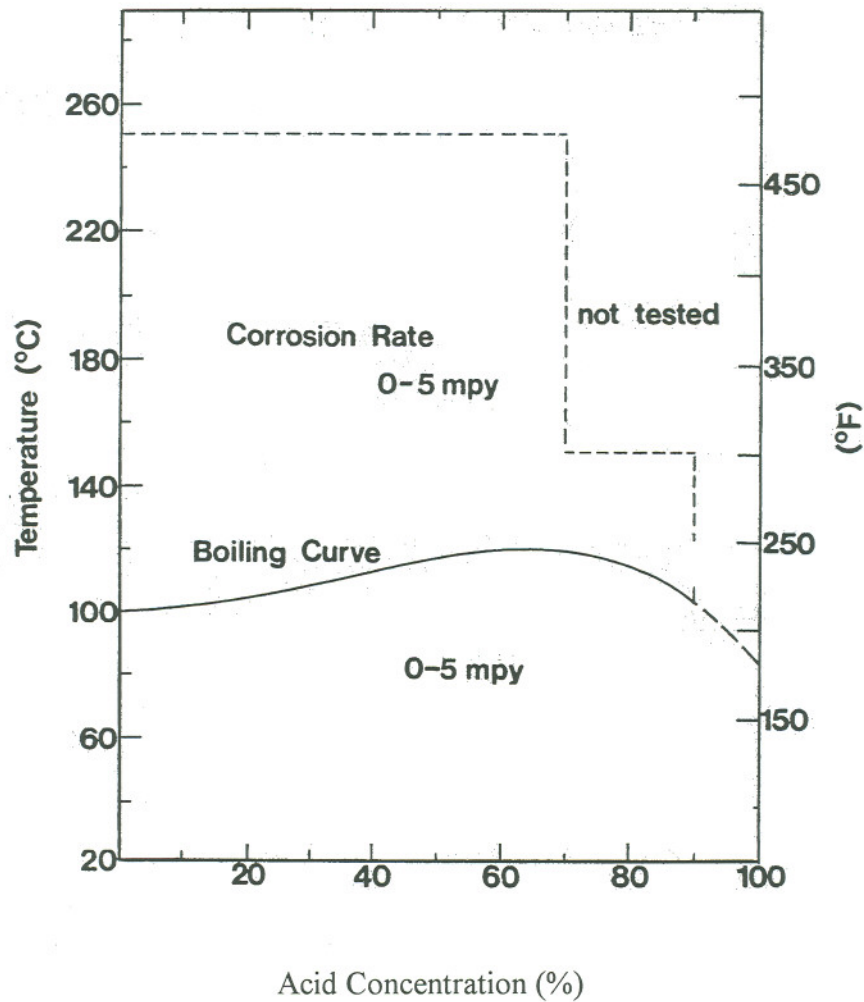


Figure 5
Isocorrosion Curve for Zirconium 702 in Nitric Acid

In the case of sulfuric acid, zirconium has very low corrosion rates at boiling temperatures when the acid concentration is below 65%. At lower temperatures, zirconium can be used to 70%. Figure 6 gives the isocorrosion diagram for zirconium in sulfuric acid.

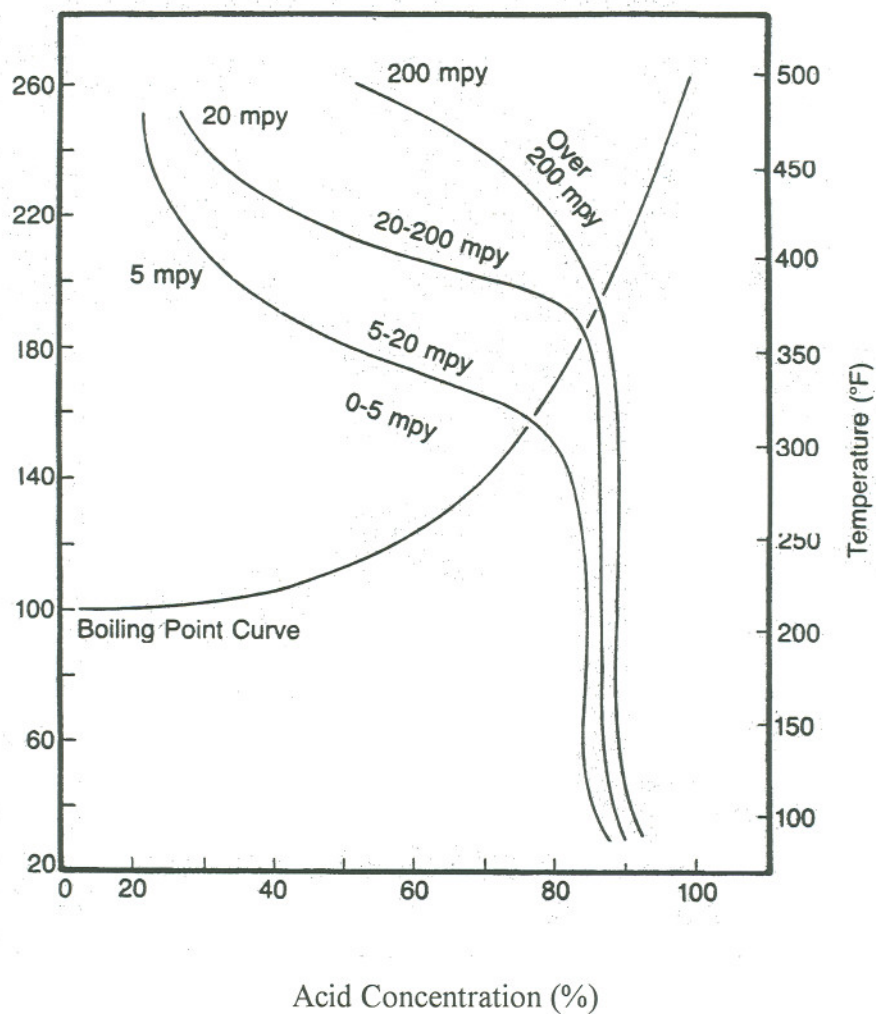


Figure 6
Isocorrosion Curve for Zirconium 702 in Sulfuric Acid

1.3.2 Neutral Solutions

Zirconium exhibits low corrosion rates in a wide range of salt solutions. Halogen, nitrate, carbonate and sulfate salts show little effect on zirconium. It should be pointed out that salt solutions containing strong oxidizing chloride solutions, such as ferric chloride and cupric chloride are among the few exceptions. Zirconium may experience high corrosion rates in these environments.

In seawater, zirconium is tolerant of wide fluctuations in environments such as pH, temperature, velocity, crevice conditions and sulfur-containing organisms. Zirconium exhibits nil corrosion in sea water even when galvanically coupled with mild steel.

1.3.3 Alkaline Solutions

Zirconium is resistant to virtually all alkaline solutions. Zirconium is resistant to corrosion in concentrated sodium hydroxide and potassium hydroxide solutions up to boiling temperatures. In concentrations up to 28%, calcium hydroxide and ammonium hydroxide do not attack zirconium at temperatures up to boiling.

1.3.4 Aqueous Organic Solutions

Zirconium is currently being used in the production of a wide range of organic chemicals. In addition to production of organics, zirconium is used in applications which require high operating temperature and high concentrations of reactants. Among these are 100% acetic acid up to 300°C, urea, 96% formic acid, hydroxyacetic acid (glycolic) to 205°C, lactic acid, methacrylic acid, alcohol and phenolic resins.[36][39] Impurities, such as copper ions can lead to pitting in certain environments such as acetic acid.

As in mineral acids, sufficient water content for zirconium to repair its passive oxide film is critical in organic environments. In organic water-soluble halides, such as trichlorethylene and dichlorobenzene, in which sufficient water (usually >50 ppm) is present, zirconium is well suited. The introduction of additional water into the system or

stress relief may be necessary for optimum performance. In water-insoluble halides, zirconium exhibits very high corrosion.[29] Zirconium is not suitable for use in organic halides that are water-incompatible.

1.3.5 Kraft Solutions

Of particular interest is the corrosion behavior of zirconium in solutions typical of the Kraft process. As seen in Table 9, a typical Kraft solution is composed primarily of NaOH and sulfur containing compounds.

Table 9 [1]
Typical Compositions of Kraft Liquors (g/L)

	Green Liquor	White Liquor	Black Liquor (45% Solids)
Sodium Hydroxide	13.0	84.0	9.4
Sulfide, as Na ₂ S	50	55.9	40.4
Polysulfide, as S _x	.25	<.04	---
Thiosulfate, as Na ₂ S ₂ O ₃	22	5.1	44.1
Sulfate, as Na ₂ SO ₄	3.7	4.4	8.7
Carbonate, as Na ₂ CO ₃	121	24.5	23.5
Chloride, as NaCl	2.2	1.7	2.2
pH	12.5	---	---
Density at 20°C (g/ml)	1.178	1.156	---

Zirconium is uniquely suited to handle these environments. In immersion testing of both welded and non-welded coupons zirconium showed a corrosion rate of less than 0.0254 mm/yr (1 mpy) at temperatures up to 225°C.[26]

With the high concentration of sulfur and sulfides present in typical Kraft solutions, thought must be given to the possibility of Sulfide Stress Cracking (SSC). Hydrogen released during the reaction between metal and sulfide ions may allow atomic hydrogen to

enter the metal lattice resulting in failure due to SSC. This severe environment is a problem for many materials of construction, but not for zirconium. Table 10 shows results for slow strain-rate tests to determine the susceptibility of zirconium to SSC in Kraft type solutions.

Table 10 [21]
Results of slow strain-rate tests of Zirconium
at 90°C and $2.5 \times 10^{-6} \text{ sec}^{-1}$

	Maximum Stress (Mpa)/Maximum Strain (%)	
	Longitudinal	Transverse
100 g/l NaOH + 33 g/l Na ₂ S	345/30.9	342/33.0
100 g/l NaOH + 33 g/l Na ₂ S + 18 g/l Na ₂ S ₂ O ₃	340/28.7	349/32.8
100 g/l NaOH + 33 g/l Na ₂ S + 18 g/l Na ₂ S ₂ O ₃ + 50 g/l NaCl	354/29.7	336/27.3
Distilled H ₂ O	---	331/27.6

Zirconium U-bends were evaluated in all three Kraft solutions. Welded and non-welded samples in four different configurations of weld orientation and metal rolling direction were tested. As Table 11 shows, no sample cracked during the 60-day test period. At the end of the 60-day test period the U-bends were over stressed to check for loss of ductility. Again no cracking was detected. The conclusion is that, under these conditions, zirconium shows no loss in the original ductility.

Table 11
Results of U-Bend tests of Zirconium 702
at 90°C for 240 days [21]

Medium	Corrosion rate		Pitting		Cracking	
	nw*	w*	nw	w	nw	w
10% NaOH	nil*	nil	no	no	no	no
20% NaOH	nil	nil	no	no	no	no
100 g/l NaOH + 33 g/l Na ₂ S	nil	nil	no	no	no	no
100 g/l NaOH + 33 g/l Na ₂ S + 18 g/l Na ₂ S ₂ O ₂	nil	nil	no	no	no	no
100 g/l NaOH + 33 g/l Na ₂ S + 18 g/l Na ₂ S ₂ O ₃ + 50 g/l NaCl	nil	nil	no	no	no	no

*nw: non-welded, *w: welded, *nil: < 25 μ m/yr

At the end of the test period, all samples were sectioned for metallographical analysis. No hydrides, pitting or cracking were observed in any of the tested samples.

1.3.6 Molten Salt

Zirconium is very resistant to corrosion in molten sodium hydroxide to temperatures of 1000°C.[29]

1.4 Wear behavior of Zirconium

Very little work has been done to characterize the wear behavior of zirconium and its alloys. Zirconium is a very soft metal with a typical hardness of 198 DPH (190 HB).[8] Zirconium is a very reactive metal. Under ambient conditions, a thin oxide film forms spontaneously. This thin oxide film accounts for zirconium's excellent corrosion resistance and, when enhanced by heat treatment, provides a hardened oxide layer more resistant to galling and abrasion.[27] A normal oxide layer, which forms at room temperature, has a typical thickness of only 100 -1000Å.[27] This oxide film will form in air, water or under oxidizing or highly reducing environment. Although protective of the surface under corrosive conditions, it is too thin to provide adequate protection from mechanical damage such as wear or galling.[27]

To thicken this protective oxide film, for providing additional protection of the surface, a high temperature treatment is required. Thicker oxide films approaching 20 μm (0.8 inches), can be formed when zirconium is heated in hot water at 360°C for 14 days, in steam at 400°C for up to 3 days, or immersion in molten salts at 600°C - 800°C for longer than 6 hours.[27] The most common method, however, is to simply heat zirconium in air at 560°C for 4-6 hours. This heat treatment gives oxide thickness of $\sim 5 \mu\text{m}$ along with an appreciable increase in hardness.[27]

Zirconium with enhanced oxide films are currently being used for pump mechanical seals, valve seats, reactor vessel walls, and agitator components. Each of these applications relies on zirconium's corrosion resistance and the protection from abrasion or galling afforded by the enhanced oxide layer.

The above methods used for increasing the oxide thickness rely on the reaction of zirconium metal with atmospheric oxygen, and is given by the following reaction.



Another, more controlled reaction, uses a constant ratio of oxygen and a diffuser gas under controlled temperatures.[28] This allows the oxide film to develop at a slower rate. The resulting thickness is ~ 0.02 mm (.0008 inches) in thickness with a hardness of 940 DPH (~ 74 HRC). The actual black oxide film developed during this process provides a hardened wear resistant surface well below the visual oxide film layer. The metal below the visual oxide film is hardened because of the diffusion of oxygen into the metallic crystal lattice. The resulting hardness of zirconium, for several thousands of an inch below the oxide film, is enhanced up to 940 DPH (~ 70 HRC).

The treatments mentioned above are performed on Zirconium 702, the commercial alloy typically used in the CPI. Additional wear information is available for Zircaloy-2, a nuclear grade of zirconium.[23] The Atomic Energy of Canada Limited, (AECL), Research Co. tested both oxidized commercial Zirconium 702 and Zircaloy-2 at 100°C and at 180°C against a variety of abrasive materials. The oxide thickness tested on Zircaloy-2 was typically 0.025 to 0.25mm (.001 to 0.010 inches) in thickness.[23] The conclusion of AECL was that oxidized zirconium, for low-speed rotational applications, was superior to stainless steel.

Haygarth and Fenwick [8] used a slurry pot testing apparatus to evaluate the susceptibility to abrasion of the oxide film developed on zirconium 702, Zircaloy-2 and Zircaloy-4. The oxide films were generated by heating in air, in fused NaCN, and in a salt bath of fused NaCl, KCl, and Na₂CO₃. This testing program showed enhanced abrasion resistance of alloys with an oxide film in comparison to un-oxidized alloys.

At the conclusion of their testing, the corrosion resistance of each alloy in boiling 70% nitric acid, 60% and 70% sulfuric acid, and 20% hydrochloric acid with 200 ppm ferric ion was determined. The corrosion rate of the alloys with the enhanced oxide films were essentially identical to the corrosion rates of zirconium with the normal spontaneously formed film. Not surprisingly, the film normally found on zirconium offers enough protect to account for zirconium's excellent corrosion resistance. No further oxide enhancement is necessary for corrosion resistance.

The oxide layer developed by Haygarth and Fenwick [8] had a thickness of 6-10 μm . In addition, the hardness, due to oxygen diffusion, extended well below the surface of the treated sample to greater than 2.54 mm (.1 inch). Table 12 shows the hardness profile from the actual surface oxide layer to a considerable distance into the metal matrix. Haygarth states that these values are probably an underestimate because of proximity to the surface.[8]

Table 12 [8]
Hardness Profile in Zirconium 702
as Result of Oxide Enhancement

Depth from surface	Hardness (HV 025)
.254 mm (.010 inches)	488
.635 mm (.025 inches)	416
1.168 mm (.046 inches)	328
1.62 mm (.064 inches)	113
2.89 mm (.114 inches)	98

Also, Haygarth et.al. [8] studied the galling resistance of the above alloys after oxidation using Schumacher's method.[34] This method involves pressing the end of a right, circular cylinder under a known load against the flat surface of a stationary block. In this configuration, the test cylinder was rotated through 360° about its axis. After each experiment, optical examination of the surface was performed to evaluate the surface for signs of galling. No evidence of galling was found.

1.5 Overview of Pulping Processes

Several processes are used for delignification. This is the initial separation of the cellulose fibers from the surrounding lignin. Each of these processes must accomplish this separation while maintaining a high yield of intact hemicellulose and cellulose components. Both requirements are critical in providing a quality product at reasonable yields and economics.

There are several pulping processes. This chapter will look at Kraft, mechanical, thermomechanical, and alkaline peroxide mechanical pulping. Another proposed method using white-rot fungus to delignify raw pulp will be mentioned.

1.5.1 Kraft Process

The Kraft, or sulfate pulping, method is the most widely used. [17] It is alkaline in nature using hydroxides, carbonates and sulfur compounds, to delignify the feedstock. For the Kraft pulping method, almost any type of wood fiber, both hard wood and soft wood, can be utilized. This feature makes Kraft pulping one of the most versatile of major pulping schemes. Cooking time is between 2 and 5 hours at a pressure of 660-925 kPa. Operating temperatures are typically 170-176°C. Along with the versatility of using a wide variety of wood types, the ability to recycle chemicals and generate operating heat by burning the black liquor waste stream makes this method extremely attractive both economically and environmentally.

During the processing steps, three Kraft liquors are generated. These are referred to as White, Black, and Green liquors. Typical chemical composition of the three Kraft liquors were given in Table 9.

White liquor is used in the initial stage of the pulping process. In this stage, lignin is dissolved from wood chips and the individual wood fibers are separated. These separated wood fibers are later used to make paper.

Black liquor is the residue formed after all the cellulose has been removed from the feed material. The residue is lignin and other organic materials in the form of alcohol and resins.[17] This black liquor waste stream is burned, in the recovery boiler, to recover contained energy values and to recycle the inorganic constituents. The equation below gives the chemical change which takes place in the recovery boiler changing Na_2SO_4 to Na_2S . [17]



The carbon needed for this reaction to take place is provided by the organics in the black liquor. This chemical, sodium sulfide Na_2S , will be recycled back into the production stream.

Green liquor forms when the smelt, the inorganic chemicals remaining after the firing of black liquor, is tapped from the bottom of the recovery boiler and allowed to fall into a weak caustic solution in the dissolver tank. Green liquor is the raw material for recycling of additional inorganic compounds used in the production of white liquor. The recovered sodium carbonate in the green liquor reacts with slaked lime according to the following equation.[17]



This reaction is the basis for recycling of Na_2CO_3 and $\text{Ca}(\text{OH})_2$ to NaOH and CaCO_3 . These inorganic components are then reconstituted and fed back to the processing stream as white liquor. This is the function of the recausticizing circuit in the Kraft pulping process. Figure 7 illustrates the recausticizing circuit.

The major product from the Kraft process is brown “Kraft” paper. These are products requiring strong fibers in the unbleached condition. Typical products include building paper, paper bags, cardboard and numerous other similar packaging products. Kraft pulp can also be bleached to product a strong white paper product. This bleaching process may, however, weaken the normally extremely strong paper fibers produced by this process.[17]

The recausticizing circuit as described above and diagrammed in Figure 7, specifically the green liquor clarifier, is the source of the green liquor used as the electrolyte for this research.

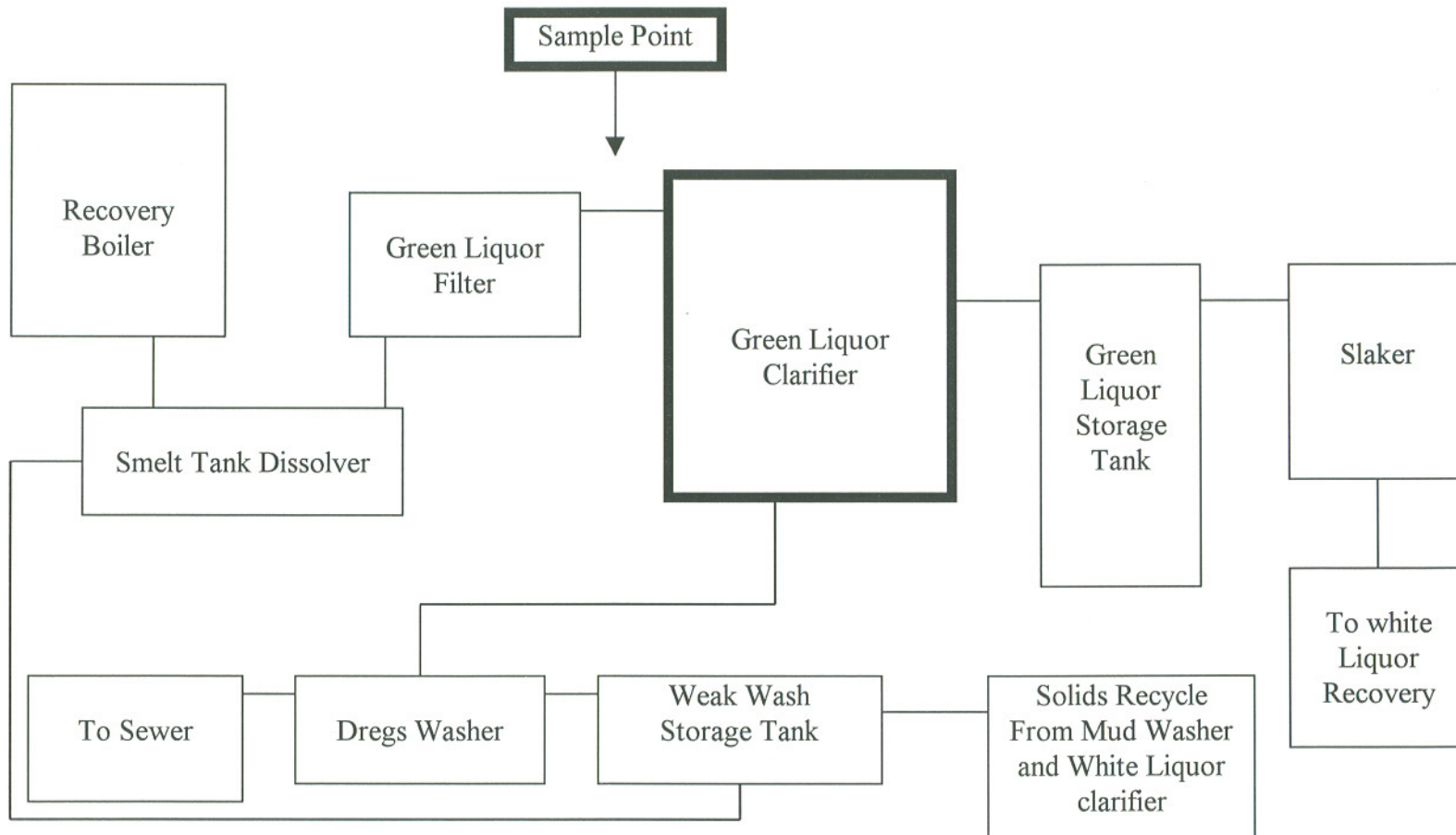


Figure 7
Diagram of Recausticizing Plant in Kraft Processing

1.5.2 Other Pulping Processes

The other pulping methods are mechanical pulping which is purely mechanical, thermomechanical in which the wood is heated before being mechanically pulped or alkaline peroxide mechanically pulped in which the wood is treated chemically before being mechanically pulped.

In purely mechanical pulping, the wood, usually softwoods such as spruce and balsam, are held against a rotating disk which tears the fibers apart producing a coarse pulp. This process uses no chemicals in the pulping process.[17]

Thermomechanical pulping is a similar process except that the grinding process takes place after the wood has been thermally treated. Pretreatment conditions are typically at 170°C and with pressures approaching 975 kPa.[17]

One step further is the alkaline peroxide mechanical pulping process. In this process wood chips are steamed and shredded, as in thermomechanical pulping, but a bleaching agent is added and allowed to penetrate the wood fibers.[12]

All of these mechanical processes produce cellulose fibers of lesser quality than those produced by the Kraft process. To increase the quality of these pulps, this lower quality pulp is often augmented by the addition of pulp produced by the Kraft process. This allows an increase in quality by improvements in strength and coloration while reducing overall cost of production.

Sulfite pulp, or acid pulping, requires a more specialized feed stock. Only coniferous species with limited chemistry and with no phenolic compounds can be used. In this process the wood is cooked for 6-12 hours at 125-160°C or higher and at a pressure of 620-755 kPa. Only sulfur dioxide is recovered for reuse. This process also produces fibers of inferior strength compared with the Kraft process.[17]

One unique approach to pulping is bioleaching using white-rot fungus IZU-154. This new approach uses a fungus to break the cellulose/lignin bond and liberate the cellulose fibers. At the same time the fungus can whiten the fibers thereby eliminating or reducing the need for the use of a bleaching agent.[14]

Sulfide pulp, or acid pulping, requires a more specialized feed stock. Only coniferous species with limited chemistry and with no phenolic compounds can be used. In this process the wood is cooked for 6-12 hours at 125-160° or higher and at a pressure of 620-755 kPa. Only sulfur dioxide is recovered for reuse. This process also produces fibers of inferior strength compared with the Kraft Process.[17]

One unique approach to pulping is bioleaching using white-rot fungus IZU-154. This new approach uses a fungus to break the cellulose/lignin bond and liberate the cellulose fibers. At the same time the fungus can whiten the fibers thereby eliminating or reducing the need for the use of a bleaching agent.[14]

Chapter 2

Research Objective

The objective of this research is to study the corrosive wear of zirconium 702 with a typical pickled surface and with an air oxidized surface. Production Green Liquor will be used for the electrolyte. Stainless Steel 304L will act as a reference material.

Chapter 3 Experimental Methods

Three different electrochemical methods were used to determine the overall and specific corrosion characteristics of the test specimens in green liquor. Each of these methods gives specific information. Actual wear testing was performed in both deionized water and green liquor. The wear testing in deionized water established the pure wear baseline.[16]

The first of these electrochemical techniques, reported in section 4.4.1, was potentiodynamic polarization. In this technique, an increasing voltage is applied to the specimen. At same time, the electrical current which is developed on the specimen surface is monitored. This technique is used to give an overall view of the corrosion behavior of the specimen in green liquor at 85°C. Corrosion potential, areas of passive and transpassive behavior and the critical current density can be determined with this technique.

Polarization resistance was the second of the electrochemical techniques used. As seen in section 4.1.2, this technique applies a small potential step to the specimen, and, after a short time interval, the current is measured. At the end of the procedure the computer generates a line with slope $\Delta E/\Delta I$. This slope is used to determine the corrosion rate of the specimen near the open circuit potential. The actual calculations are given by the Stern Geary Equation and Faraday's law. Both of these equations are given on page 53 of this thesis.

The last electrochemical technique, reported in section 4.1.3, used was monitoring of the specimen's open circuit potential in green liquor at 85°C. Monitoring the change in potential, developed on the surface of the specimen, provides information to determine if the specimen is becoming more active or less active over time.

The equipment used for all anodic potentiodynamic polarization scans, linear polarization and open circuit potential experiments was a Gamry Electrochemical System with CMS 100/105 DC software. The resulting electrochemical plots were generated by the Gamry system using Microsoft Excel.

The test electrolyte was contained in a 2000 ml Teflon corrosion cell. A three electrode setup was used for all testing. Platinum foil was used for a counter electrode, a Saturated Calomel Electrode (SCE) was used for the reference electrode. The working electrode was the test specimen. The arrangement for the three electrode corrosion cell is illustrated in Figure 8. The working electrode configuration is illustrated in Figure 9.

The potentiodynamic scan was started 0.05 volts below the open circuit potential and continued up to 4.0 volts in the anodic direction. The open circuit potential was established after 30 minutes immersion at 85°C. The scan rate was 0.2 mv/sec. All electrochemical testing was conducted at 85°C in a non-deaerated, static solution. A Luggan probe salt bridge filled with potassium chloride was used to protect the SCE glass frit from the test electrolyte and to maintain the reference electrode at near room temperature. The tip of the Luggan probe, which was immersed in the solution, was a platinum wire imbedded in glass. A water cooled reflux condenser insured consistency of the test solution. A Teflon coated type K thermocouple was used to control the heating mantle.

The sequence of operations for the electrochemical testing was as follows: The non-deaerated electrolyte was brought to the working temperature of 85°C. The platinum counter electrode, and the Luggan probe holding the SCE were already in place. Once the electrolyte was at the working temperature of 85°C, the prepared working electrode was introduced. Specimen preparation is given in section 3.1.1. The specimen was held in the electrolyte for 30 minutes before the electrochemical experiment was started. This time delay allowed the test specimen to stabilize at the open circuit potential. Fresh electrolyte were used for each experiment.

The use of Teflon was necessary due to high pH (pH 12-13) of the test electrolyte. With the exception of the Pt/glass tip of the Luggan probe, only Teflon and the test specimen were allowed to come into contact with the test electrolyte.

All wear testing was performed on an ISC-200 Tribometer. Data acquisition was provided by an IBM PC computer. Figure 10 gives a generalized view of the experimental setup. Friedersdorf and Holcomb [2] give an excellent description of the experimental procedure and equipment. The abrasive used was a 240 grit aluminum oxide abrasive disk. The machined sample pins were ultrasonically degreased in acetone, rinsed in ethanol and finally rinsed in deionized water. The samples were then weighted to 0.01 mg. After weighting, the sample pin was placed into the sample holder in such a way as to be able to remove the samples after a set number of revolutions and then replace the sample into the same orientation for further testing. A calibration block was used to ensure uniformity in the surface expose of the sample pin for each test period. An exposure of 6.3 mm (0.125 inches) of sample pin was allowed to extend beyond the Teflon sheath which covers the actual sample holder. The sample holders for each material were machined of a like material to reduce the effects of galvanic corrosion.

Specimens and the abrasive disk were broken-in before actual testing. Break-in is a process to mate the abrasive surface to the test pin. In each case, the break-in distance was 10 meters in DI water at room temperature. The normal force was 1.4 Newtons and the sliding speed was 0.1 m/s. After break-in, the paired abrasive disk track and the corresponding test pin were used for actual testing. Additionally, because of the high corrosion rate of aluminum oxide in high pH solutions, each disk was used for only one set of wear testing and then discarded. In the case of oxidized zirconium test pins, the nonoxidized pins were first then oxidized as described in section 3.1.2.

To determine pure wear, test pins were run in DI water at 85°C similar to the method used by Schumacher [16]. In the absence of any corrosion, the weight loss exhibited by the test pins can be attributed to pure wear. In other studies [9] and in ASTM recommended practice G-119 [3], a potential cathodic to the open circuit potential is applied to the test pin to eliminate any weight loss due to corrosion. Under cathodic protection, any measured weight loss would be attributed to pure wear. In the case of zirconium with an oxidized surface this is not practical considering the arrangement of the test equipment. The high dielectric constant of the zirconium oxide layer, specific

electrical resistance 10^{13} - 10^{14} ohm-cm [40], makes adequate electrical contact difficult or at best unreliable.

The electrolyte was constantly recirculated through the heated 2000 ml Teflon reservoir to the test bowl. The temperature was monitored in the test bowl near the test pin. Peristaltic pumps maintained the test bowl volume at 400 ml with a flow rate was 350 ml/min. The bowl volume and the flow rate of 350 ml/min gives a refresh rate of 1.1 bowl volumes per minute. The electrolyte inlet was approximately 13 mm (0.5 inches) up wheel of the sample. Corrosive wear product was allowed to settle out in the bottom of the reaction bowl.

Fixed conditions for each test material included the normal force of 1.4 Newtons (N), sliding speed of 0.1 m/s, solution composition and the solution temperature. Variables were sliding distance and pin material.

Wear testing involves contacting the specimen, under a known load, against a rotating abrasive disk. The disk and the specimen are immersed in the electrolyte and maintained at the test temperature of 85°C . The volume change per distance traveled, on the abrasive disk, is calculated by knowing the change in weight of the specimen and the specimen density. Wear rates are expressed in mm^3/meter . A generalized diagram of the wear testing apparatus is depicted in Figure 10.

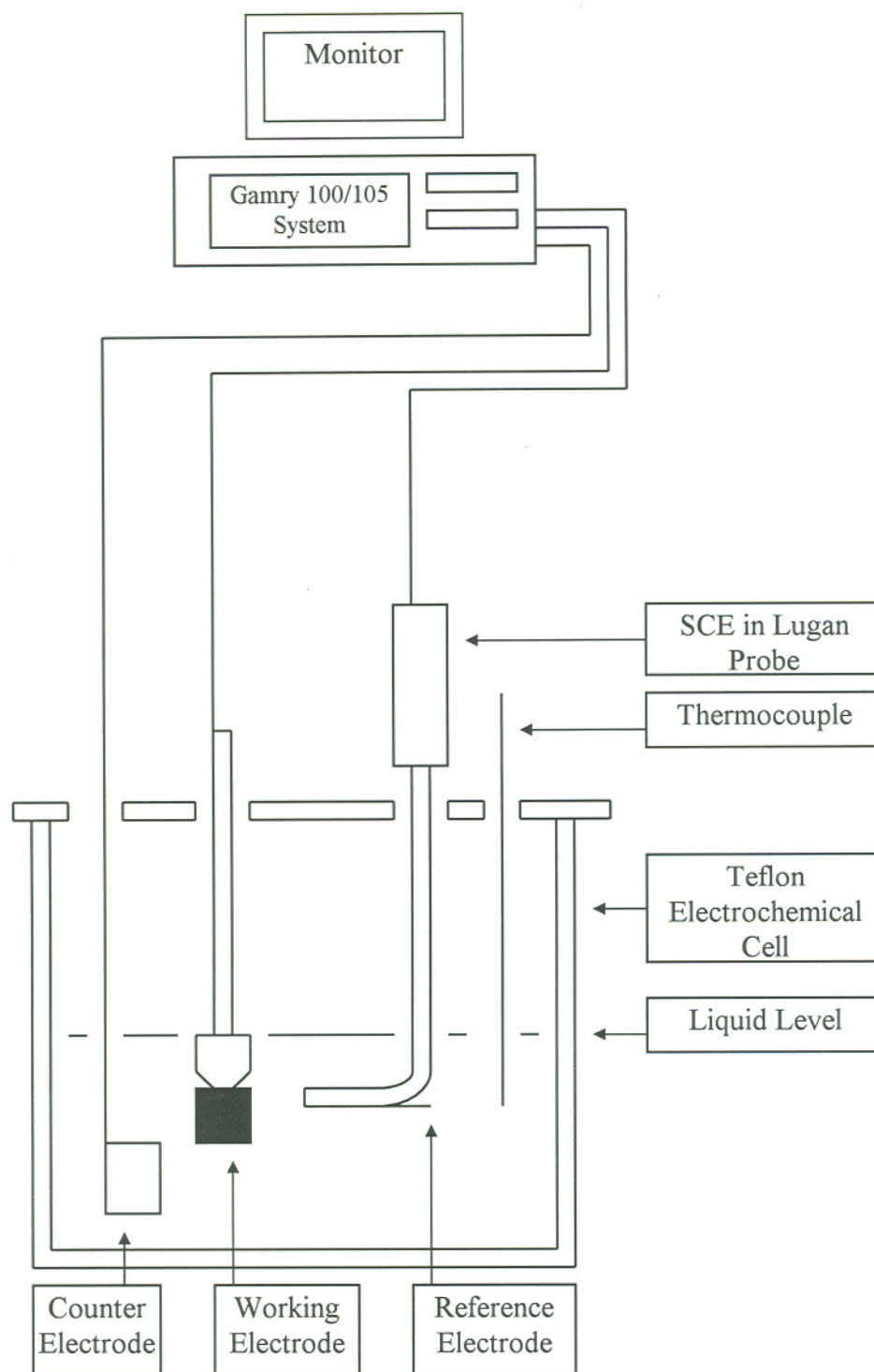


Figure 8
Generalized Diagram of Electrode Placement
and Electrochemical Cell Setup

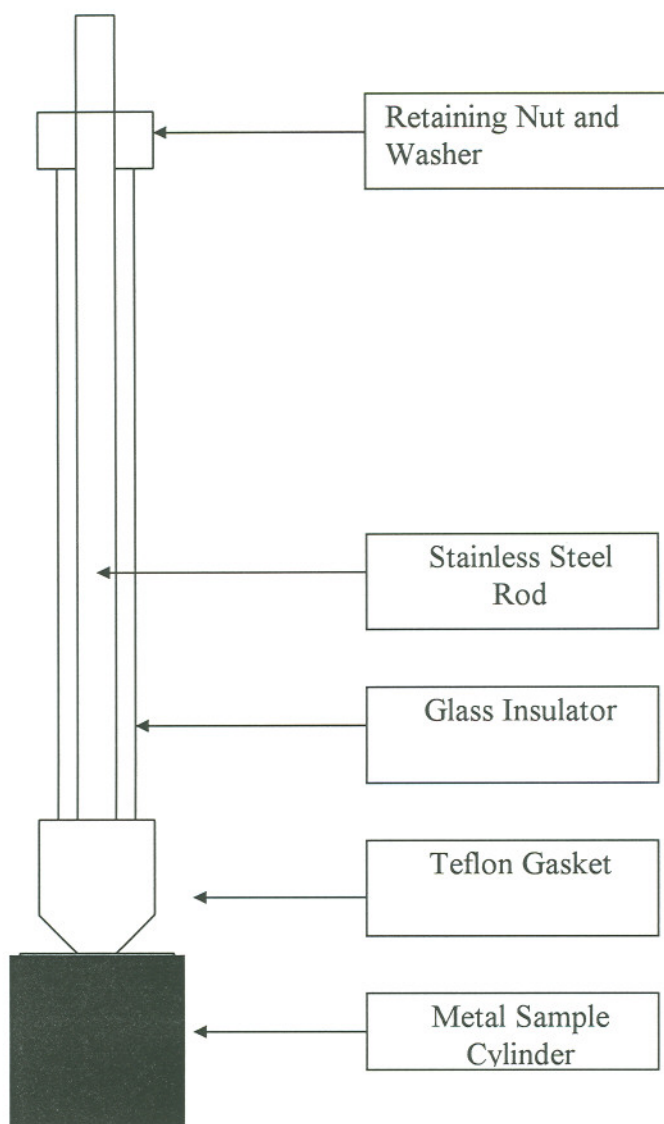


Figure 9
Working Electrode Configuration

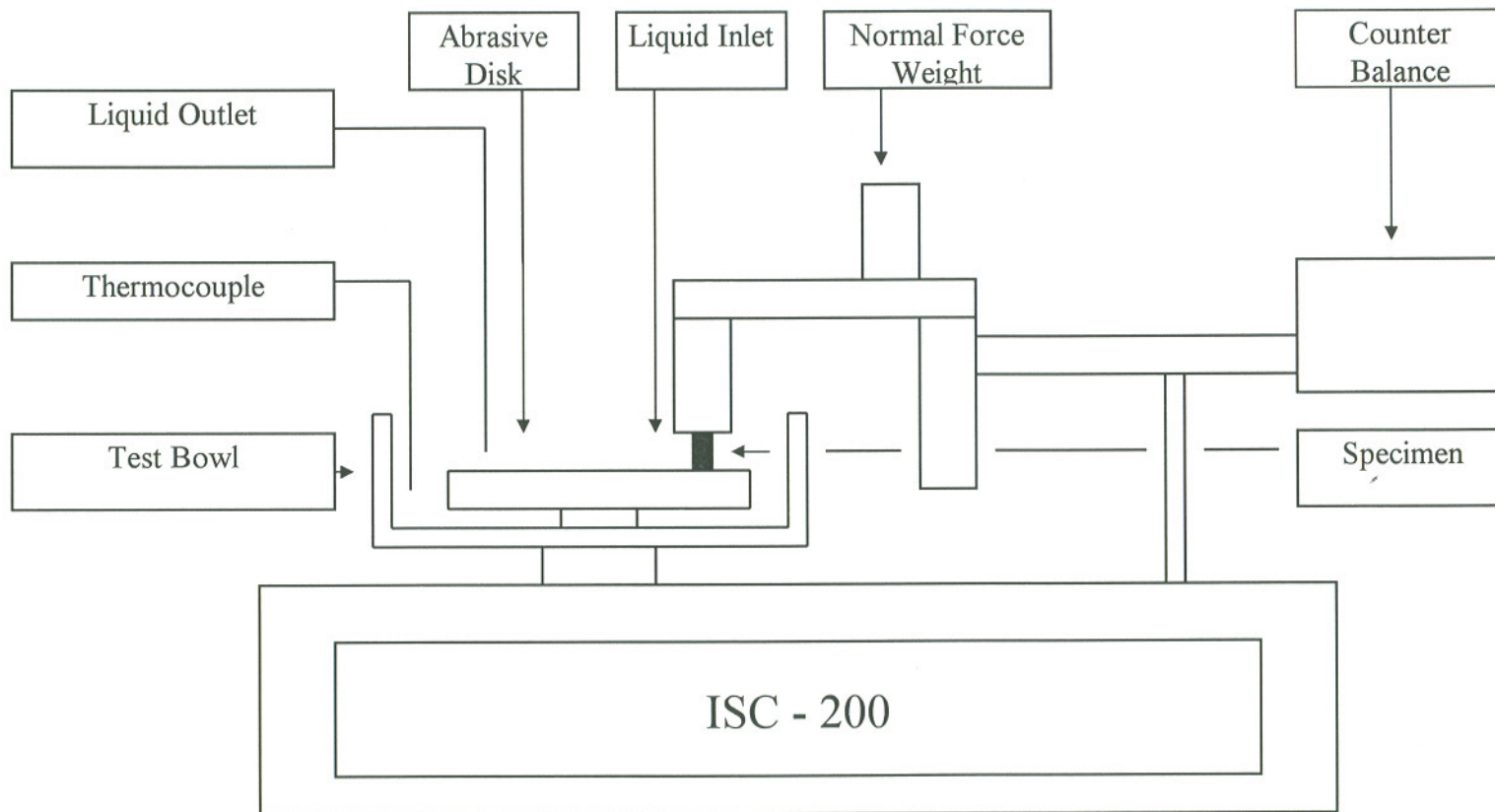


Figure 10
Generalized Diagram of Wear Test Apparatus

3.1 Materials

3.1.1 Electrochemical Specimens

Electrochemical specimens were cylinders of Zr 702 rod. Dimensions were 12.7 mm long and 12.7 mm in diameter (0.5 inches x 0.5 inches) drilled and taped to fit onto the working electrode holder, see Figure 9. These samples were wet ground with 600 grit silicon carbide paper, and pickled in a mixture of 3.0% hydrofluoric acid and 39% nitric acid with the remainder being distilled water. This procedure follows ASTM standard G-2.[18] The oxidized samples were pickled as described above and then air oxidized at 566°C for 4 hours.

The chemical composition and initial hardness of the specimens used for electrochemical testing are given in Tables 13 and 14 respectively.

Stainless Steel 304L electrochemical samples were cylinders machined from typical production rod to the same dimensions as the zirconium specimens, namely 12.7 mm long and 12.7 mm in diameter, (0.5 inches x 0.5 inches). These samples were abraded with 600 grit wet silicon carbide paper following the procedure in ASTM standard G-5.[19] No additional surface preparation was used.

3.1.2 Wear Specimens

Zr 702 and SS 304L rod 3.17mm (0.125 inches) in diameter and 15.9 mm (0.625 in) in length were used for all wear test specimens. Wear specimens, with the exception of the oxidized zirconium specimens, were first machined to size and then broken-in for a distance of 10m. This break-in period resulted, for both the SS 304L and the nonoxidized zirconium, in identical wear surfaces for both specimen types. In the case of the oxidized zirconium specimens, the samples were first broken-in, as described above, then oxidized.

Composition of specimen material used for wear testing and their initial hardness values are given in Tables 13 and 14.

Table 13
Actual Composition of Test Specimens
(Weight percent)

Electrochemical Specimens

Zr 702 Zr >99, Fe+Cr <.1, Hf .15 H .0015, N .0029, O .1350

Wear specimens

Zr 702 Zr >99, Fe+Cr .09, Hf 1.0, H .009, N .0044, O .1425

SS 304L .02 C, 18.26 Cr, .30 Cu, 1.86 Mn, .30 Mo, 8.11 Ni, .032 P, .002 S,
.56 Si, .09 N. balance is Iron.

Table 14
Initial Hardness

Zr 702	Specimens	HV (1 kg)	74
Zr 702 Oxide	Specimens	HV (025)	488 [8]
SS 304L	Specimens	HV (1 kg)	102

Oxidized Zr 702 samples were generated from the same lot of material as the non-oxidized specimens but specially prepared for testing. These samples were wet ground with 600 grit silicon carbide paper, and pickled in a mixture of 3.0% hydrofluoric acid and 39% nitric acid with the remainder being distilled water (ASTM standard G-2).[18] Specimens were broken-in for a distance of 100 meters. Specimens were then heated in air at 566°C for 4 hours.

Stainless Steel 304L specimens were machined from 3.17 mm (0.125 inches) rod. Specimen composition is given in Table 13; initial hardness are given in Table 14. Samples were machined 15.9 mm (0.625 inches) in length. No special surface preparation was used. In the case of the stainless steel specimens, both the electrochemical and the wear specimens were machined from the same lot of rod material.

3.1.3 Electrolyte

Initial break-in and generation of samples for microhardness determination were generated in deionized water.

Production filtered “clean” green liquor obtained from a local production source was used for all actual testing. Typical compositions of green liquor and actual dissolved metal ion concentrations are given in Table 15 and Table 16 respectively.

Table 15 [1]
Chemical Composition of Typical
Commercial Green Liquor
(g/ml)

Sodium Hydroxide	13.0
Sulfide, as Na ₂ S	50
Polysulfide, as S _x	.25
Thiosulfate, as Na ₂ S ₂ O ₃	22
Sulfate, as Na ₂ SO ₄	3.7
Carbonate, as Na ₂ CO ₃	121
Chloride, as NaCl	2.2
pH	12.5
Density at 20°C (g/ml)	1.178

Table 16
Actual Dissolved Metallic Ions in
Production Green Liquor
(mg/l)

Aluminum	32
Manganese	0.4
Molybdenum	0.26
Calcium	24
Silicon	469
Phosphorus	28
Sulfur (by gravity method, reported in g/l)	74

Cobalt, copper, chrome, iron, nickel, zinc, and titanium all reported back as < .01 mg/l.

Before actual testing, a simple test was performed to determine if any volatile sulfur compounds, such as hydrogen sulfide, would be evolved during testing. This could change the chemistry of the test electrolyte. In this test, 500 ml of green liquor was heated at 85°C for 4 hours. The container containing the electrolyte had the same surface area exposure as the test bowl in the corrosive-wear apparatus. The sulfur content was determined before and after the test. After chemical analysis, no difference could be detected in the sulfur concentration. This simple test indicated the relative stability of the sulfur compounds during the test period of a typical corrosive-wear experiment.

The consistency of the solution chemistry was estimated by measuring solution pH change over time. The refrigerated solution was warmed to room temperature and the pH measured. The solution was then heated at 85°C for a 4-hour period. The sample was allowed to cool to room temperature and the pH was measured again. No change in pH was detected.

Chapter 4 Results and Discussion

4.1 Experimental Results

4.1.1 Potentiodynamic Polarization Experiments

Potentiodynamic Polarization experiments were performed on all specimens in green liquor at 85°C.

The anodic polarization curve for Zr 702 with a pickled surface treatment is shown in Figure 11. This curve shows two passive regions. The first passive region is well defined, it extends approximately 0.9V (SCE) from -0.9V up to 0.0V. The current density of this area is approximately 0.01 $\mu\text{A}/\text{cm}^2$. The second passive region is reached at higher voltages of 4.0V and beyond. The current density at this point is approximately 0.10 mA/cm^2 . In both cases, the passive region could be attributed to the development of a ZrO_2 surface film. The differences in voltage may indicate a difference in crystalline structure of the surface oxide.

After the formation and breakdown of the first passive region the anodic polarization curve indicates a transpassive region. This transpassive region continues until reaching the primary passive potential (E_{pp}) of approximately +0.9V. At this point, the critical passivation current of 0.4 mA/cm^2 is reached. From this point onward the anodic polarization curve indicates the surface is repassivating, reaching its second passive region as described above.

The anodic polarization curve for zirconium 702 with an air oxidized surface treatment is shown in Figure 12. As expected, this curve shows a relatively smooth curve starting at the open circuit potential of approximately -0.7V and extending up to the final voltage of +4.0V. The maximum current density reached is 0.06 mA/cm^2

The anodic polarization curve for Stainless Steel 304L is shown in Figure 13. In this environment, SS 304L exhibits an active region extending from the open circuit potential to the primary passive potential of approximately -0.9V. At this voltage (E_{pp}) the critical passivation current is 40 mA/cm^2 . After reaching the critical passivation current, SS 304L reaches a passive region extending from approximately -0.3V to -0.25V. Following this passive region, the anodic polarization curve indicates that SS 304L exhibits transpassive behavior until the current limit of the measuring instrument is reached at 1.0A.

Anodic polarization scans for all three specimen materials were performed three times to ensure reproducibility.

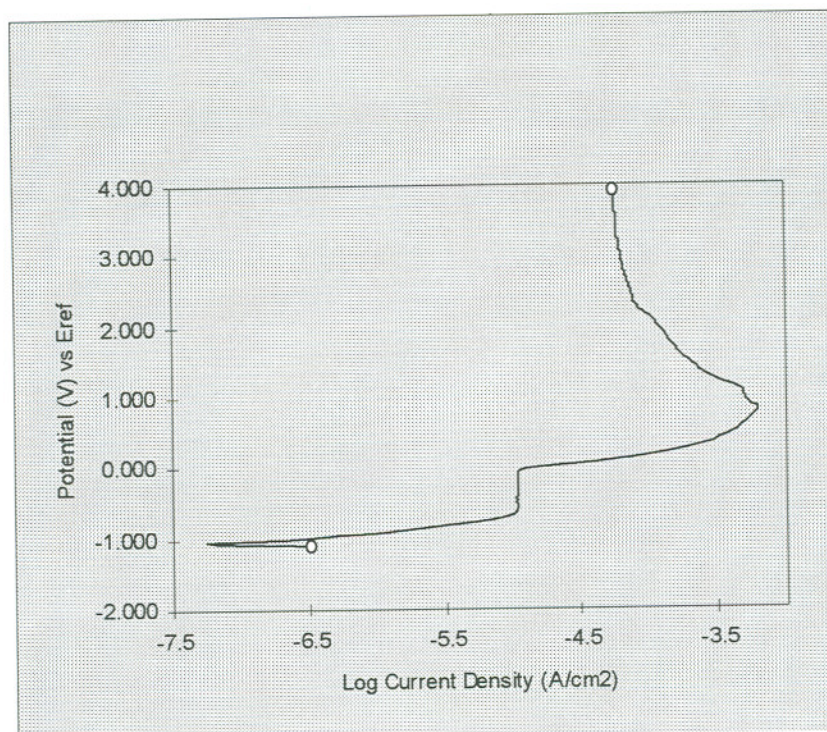


Figure 11
Anodic Polarization of
Zirconium 702 with Pickled Surface in Green Liquor at 85°C
Scan Rate 2 mv/sec

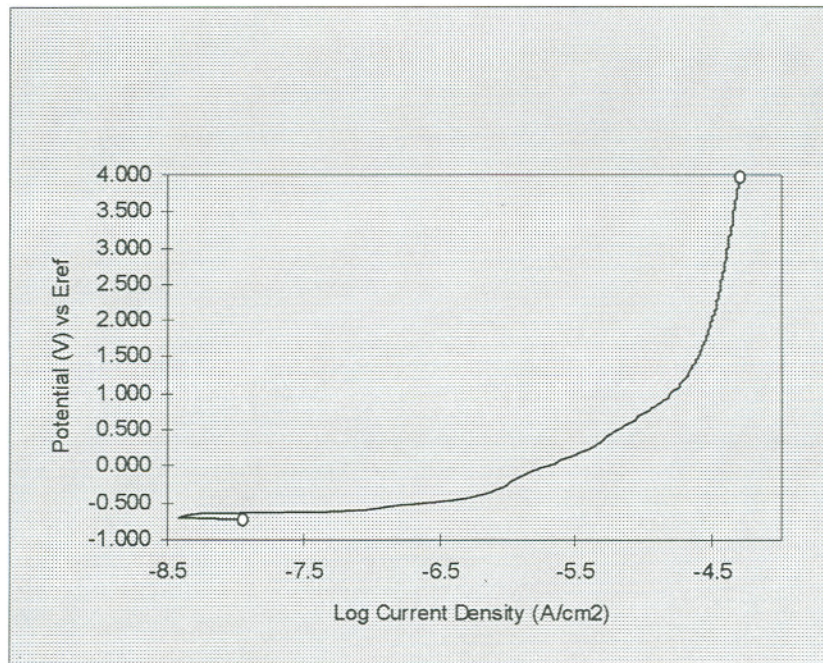


Figure 12
Anodic Polarization of
Zirconium 702 with Oxidized Surface in Green Liquor at 85°C
Scan Rate 2 mv/sec

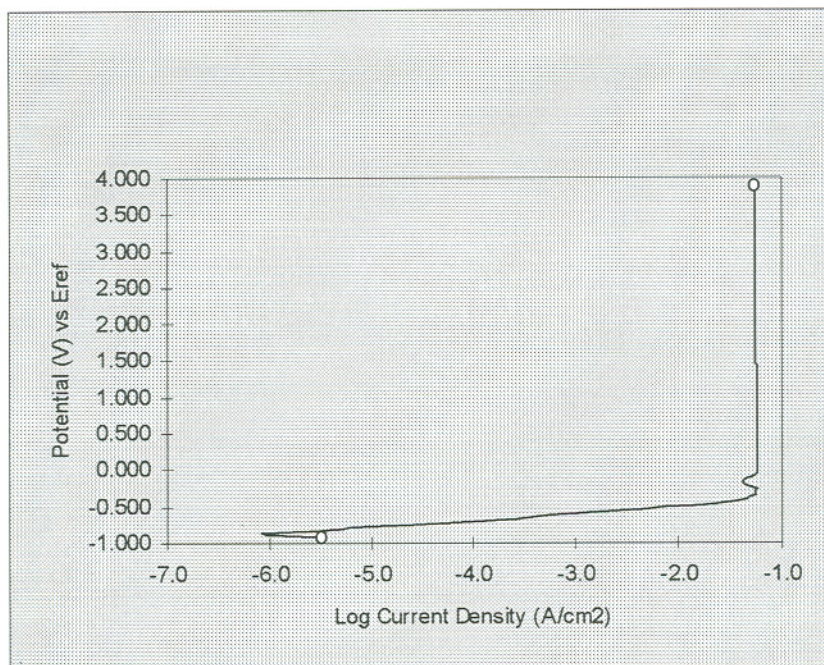


Figure 13
Anodic Polarization of
SS 304L in Green Liquor at 85°C
Scan Rate 2 mv/sec

Figure 14 shows the effect of surface treatment on the anodic polarization curves of Zr 702 in green liquor at 85°C. This figure indicates that after scanning from -0.05V (SCE) through 4.0V, even with different surface treatments and different initial open circuit potentials, Zr 702 reaches the same final current density of approximately 0.32 mA/cm².

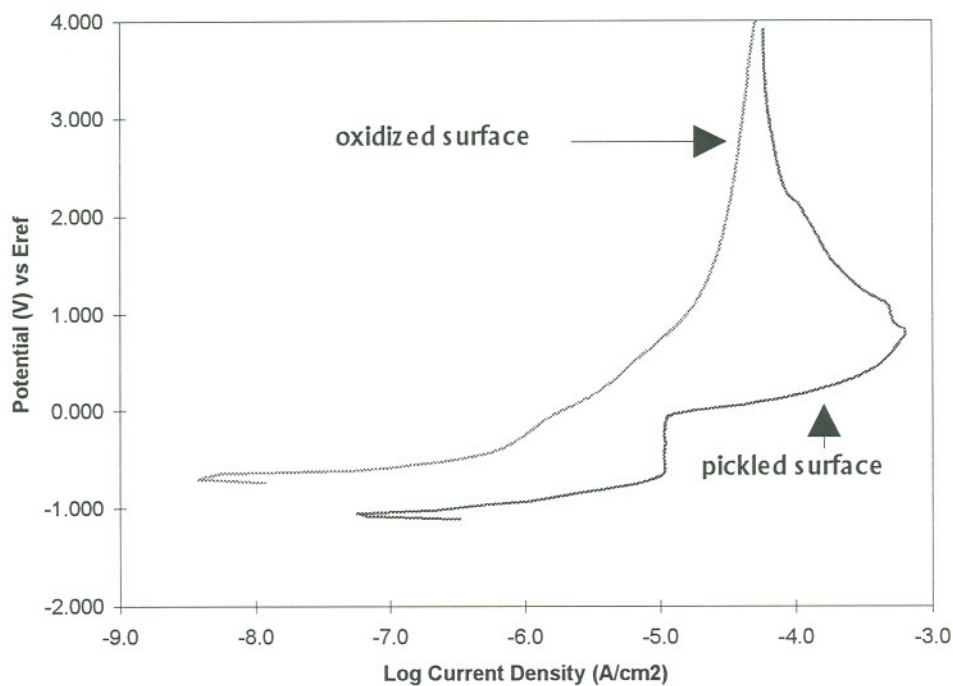


Figure 14
Anodic Polarization Curves
The Effect of Zirconium 702 Surface Treatment
In Green Liquor at 85°C
Scan Rate of 2 mv/sec

4.1.2 Polarization Resistance Experiments

Figures 15 and 16 show the results of the polarization resistance experiments, also known as linear polarization, of Zr 702 with a pickled surface treatment and with an oxidized surface treatment in green liquor at 85°C. SS 304L results, also in green liquor, are reported in Figure 17.

Linear polarization provides data to determine the slope, $\Delta E/\Delta I$, over the range of ± 20 mv to the open circuit potential. This slope is represented as the linear line on Figures 15, 16 and 17. The Tafel constants, β_a and β_c , are derived from reasonable estimates of +.12V and -.12V respectively.[41][7] For the final calculation of corrosion current, i_{corr} , the Stern Geary Equation [7] is used according to the following equation.

$$\Delta E/\Delta I = \beta_a \beta_c / 2.3 [i_{corr}] [\beta_a + \beta_c] \quad [41]$$

Once the corrosion current is determined, as outlined above, the corrosion rate (mpy) can be determined by using Faraday's Law.[7]

$$\text{Corrosion Rate (mpy)} = 0.13 i_{corr} (\text{Equivalent Weight}) / \text{Density} \quad [41]$$

The 0.13 proportionality constant is used to calculate the corrosion rate in mils per year (mpy). A proportionality constant of .000327 is used for determining the corrosion rate in millimeters per year (mm/yr).

The final corrosion rate data for zirconium 702 and SS304L in green liquor at 85°C is presented in Table 17. Two sets of data are presented to indicate the data reproducibility.

Table 17
Polarization Resistance in
Green Liquor at 85°C

	First Experiment	Second Experiment
Zirconium with Pickled Surface Treatment		
Corrosion Rate (mm/yr-mpy)	.0018 - .071	.00145 - .057
I_{corr} (A/cm ²)	1.6×10^{-7}	1.2×10^{-7}
Zirconium with Oxidized Surface Treatment		
Corrosion Rate (mm/yr-mpy)	.0001 - .004	.00008 - .003
I_{corr} (A/cm ²)	8.4×10^{-9}	6.1×10^{-9}
SS 304L		
Corrosion Rate (mm/yr-mpy)	.0087 - .343	.0062 - .245
I_{corr} (A/cm ²)	8.4×10^{-7}	8.3×10^{-7}

Table 17 shows that zirconium with the oxidized surface treatment has the lowest corrosion rate whereas SS 304L has the highest. These results for zirconium are in good agreement with corrosion rates for zirconium in other similar electrolytes, such as white liquor.[26]

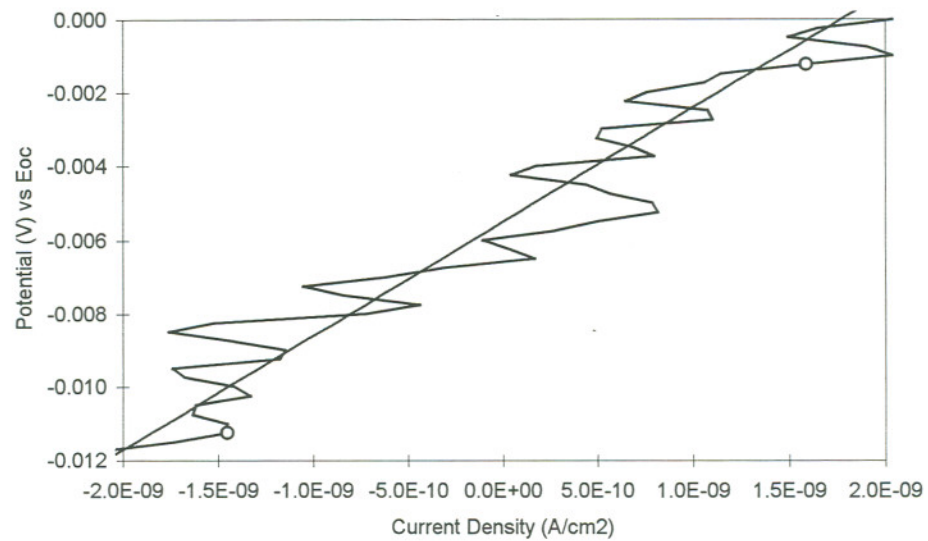


Figure 15
Polarization Resistance of
Zirconium 702 with Pickled Surface in Green Liquor at 85°C

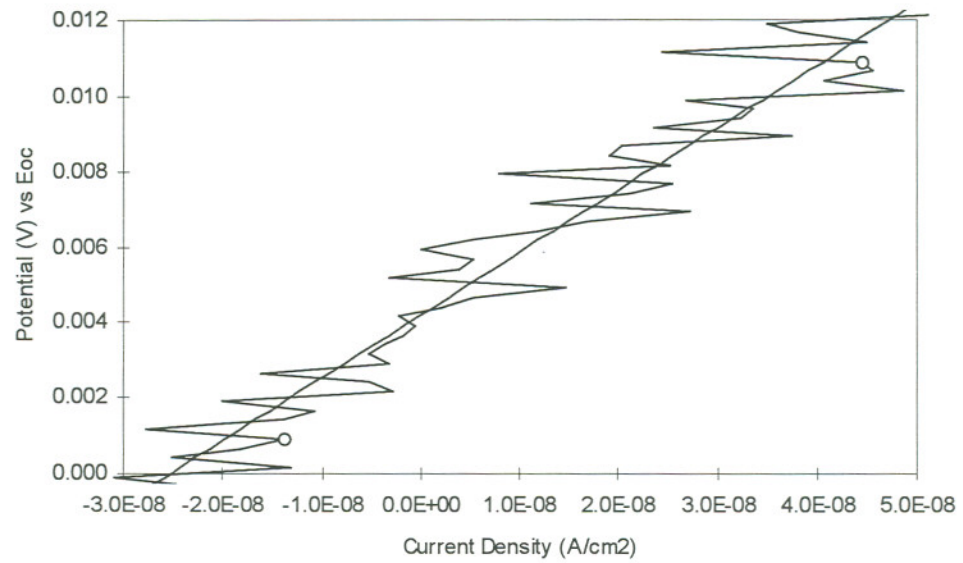


Figure 16
Polarization Resistance of
Zirconium 702 with Oxidized Surface in Green Liquor at 85°C

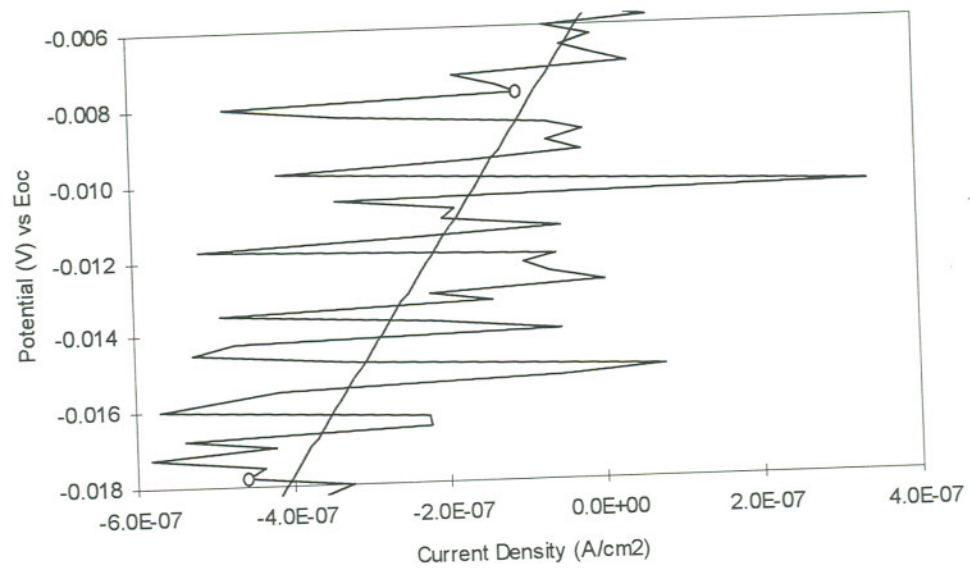


Figure 17
Polarization Resistance of
SS 304L in Green Liquor at 85°C

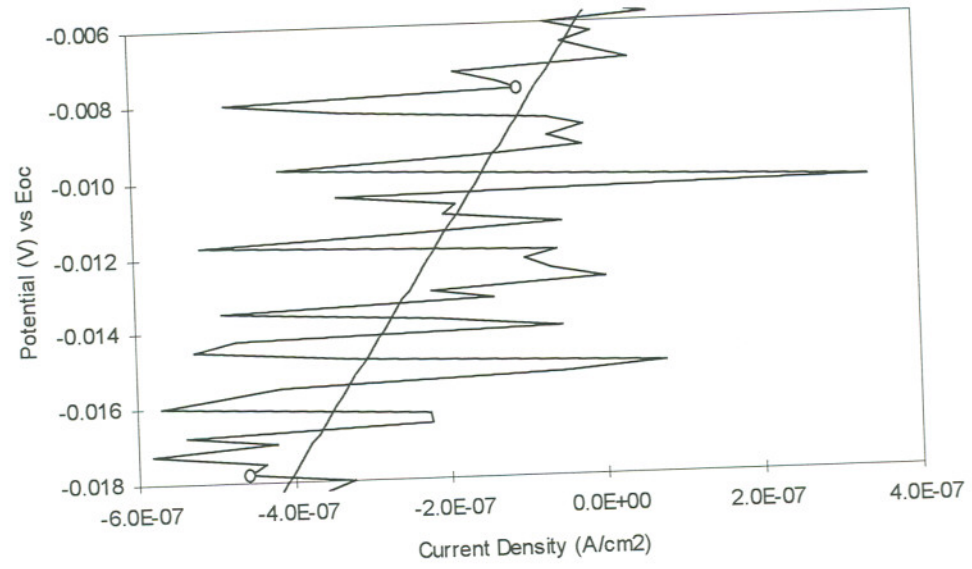


Figure 17
Polarization Resistance of
SS 304L in Green Liquor at 85°C

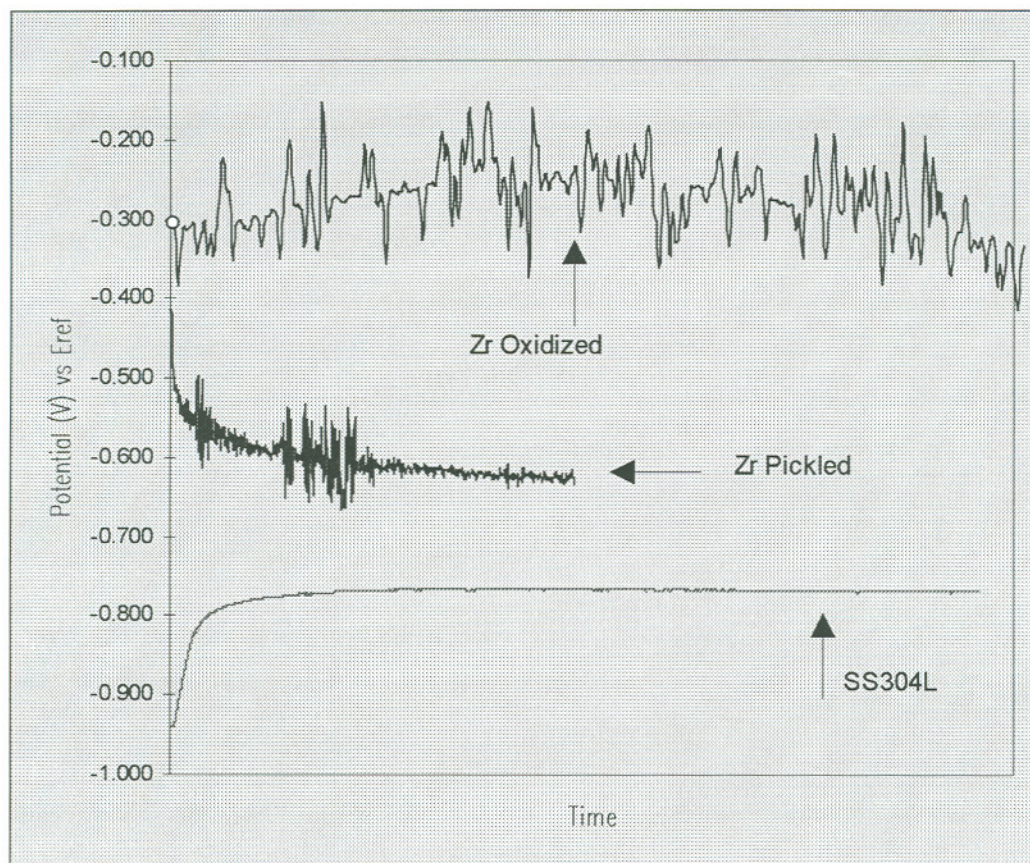


Figure 18
Comparison of Open Circuit Potentials
Zirconium 702 with Pickled Surface Treatment,
Zirconium 702 with Oxidized surface Treatment, and
SS 304L in Green Liquor at 85°C

4.1.4 Wear Experiments

Wear experiments were run in deionized (DI) water at 85°C. Since zirconium is highly resistant to corrosion in water, any resulting volume loss can be attributed to the result of pure wear. Figures 19, 20 and 21 give the volume change of zirconium with a pickled surface treatment, zirconium with an oxidized surface treatment and stainless steel 304L, respectively. Figure 22 shows a direct comparison of volume loss for the zirconium surface treatments.

The calculations for volume loss for zirconium with the pickled surface treatment and the zirconium with an air oxidized surface treatment did not adequately demonstrate the differences between the two samples. Figure 19 for the pickled surface and Figure 20 for the oxidized surface show very little difference. Only a slight variation is noticeable in the graph for the specimen with the oxidized surface as compared with the specimen with the pickled surface. This difference, as expected, is more noticeable in the first 5 meters of wear testing when compared to the 5 to 10 meter tests. This is the region where the oxide film is still intact. Once the oxide layer is removed, after the first 5 meters, the softer zirconium base metal is being abraded.

The graphical results for the wear data, Figures 23 and 24, make the difference between the two surface treatments for zirconium much more apparent. As expected and shown in Figure 24, zirconium with an oxidized surface treatment had better wear resistance, approximately $0.0065 \text{ mm}^3/\text{m}$, for the initial contact period of 1 to 5 meters sliding distance. However, as shown in Figure 24, after about 5 meters sliding distance the oxide layer and the associated oxygen strengthened sublayer was worn off. As expected, after the oxide film and the underlying oxygen hardened layer was removed, the two types of specimens exhibited nearly identical wear rates. Figure 24 shows that the wear rate for the pickled surface and for the oxidized surface after 5 meters is approximately $0.0085 \text{ mm}^3/\text{m}$. Also, once the oxide film and the hardened sublayer was removed, the remaining oxide formed on the walls of the specimen did not significantly affect the wear resistance.

It was surprising that zirconium with a pickled surface treatment, being a considerably softer metal, had the same wear rate as SS 304L in DI water. Longer sliding distance testing of zirconium at 50, 100 and 250 meters confirmed the wear rate of 0.008 mm³/m for zirconium with the pickled surface treatment. Long sliding distance wear testing of SS 304L of 15 and 25 meters resulted in wear rates of 0.007 mm³/m.

One possible explanation of the unexpected wear resistance of Zr 702 could be the tendency of zirconium to work harden. As can be seen in Table 18, however, the hardness before a 100m break-in period is very similar to the hardness after the break-in period. The SS 304L specimens showed similar results with very little difference between the 100m break-in period and the specimens without any break-in period. Work hardening does not appear to account for the wear resistance of zirconium.

Table 18
Affect of 100m break-in on
Hardness

Zr 702	saw cut	76 HV	(1 kg)
	abraded	74 HV	(1 kg)
SS 304L	saw cut	102 HV	(1 kg)
	abraded	108 HV	(1 kg)

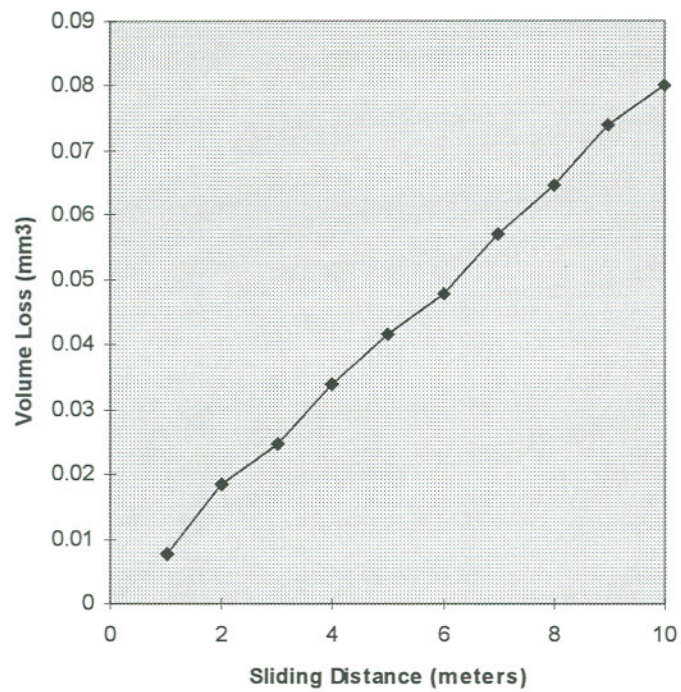


Figure19
Volume Loss Vs Sliding Distance of
Zirconium 702 with Pickled Surface Treatment
in DI water at 85°C

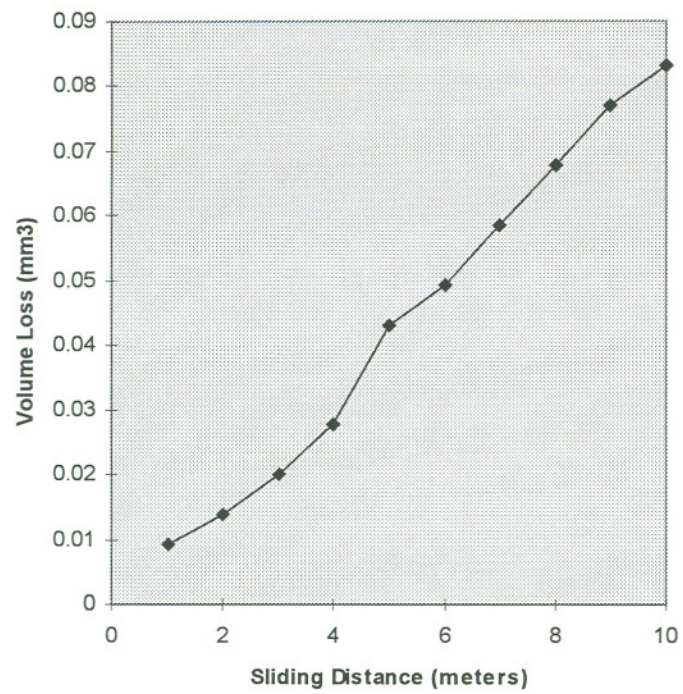


Figure 20
Volume Loss Vs Sliding Distance of
Zirconium 702 with Oxidized Surface Treatment
in DI water at 85°C

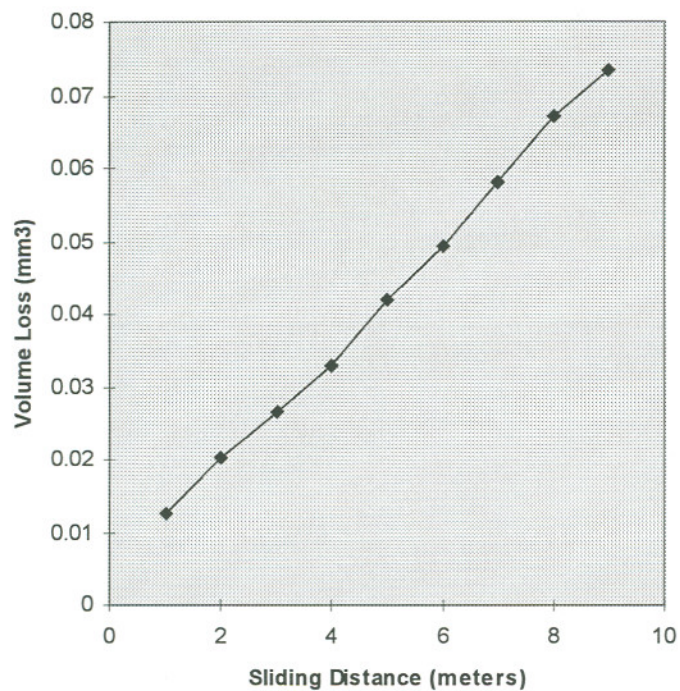


Figure 21
Volume Loss Vs Sliding Distance of
Stainless Steel 304L
in DI water at 85°C

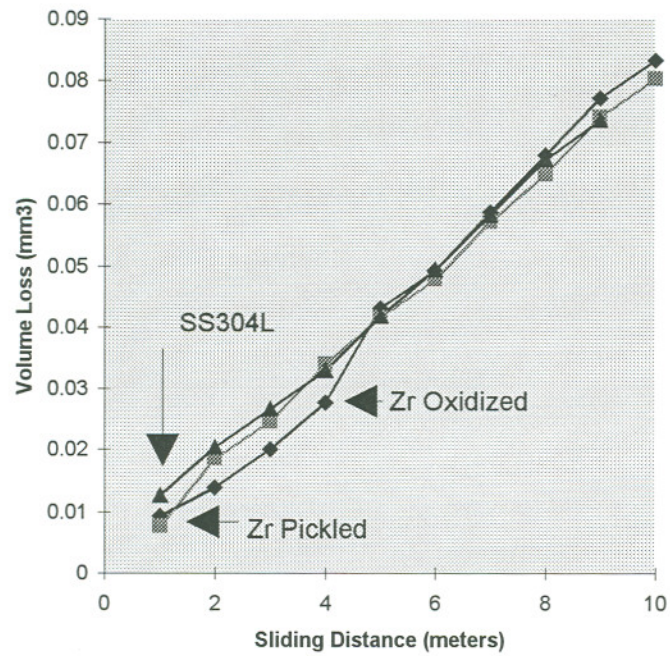


Figure 22
Comparison of Volume Loss Vs Sliding Distance of
Zirconium 702 with Pickled Surface Treatment,
Zirconium 702 with Oxidized Surface Treatment and
Stainless Steel 304L
in DI water at 85°C

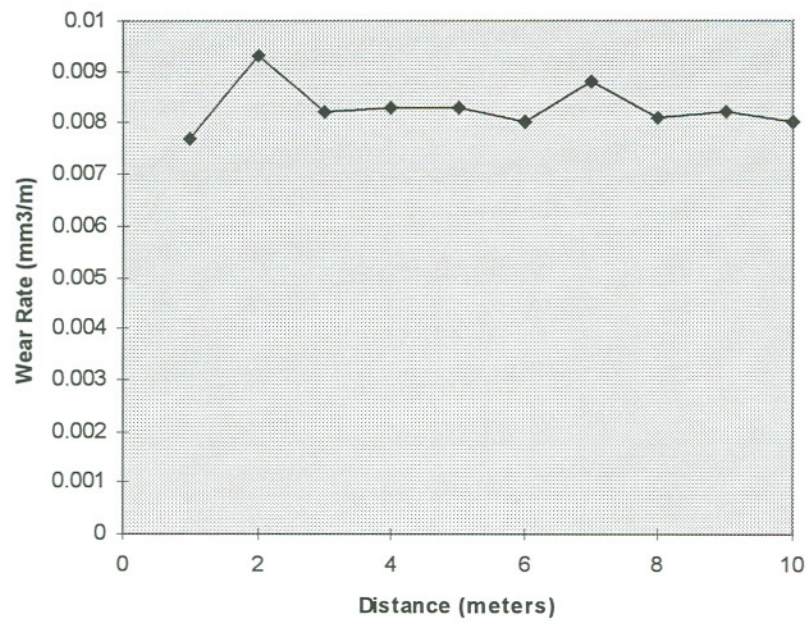


Figure 23
Wear Rate Vs Sliding Distance of
Zirconium 702 with Pickled Surface Treatment
in DI water at 85°C

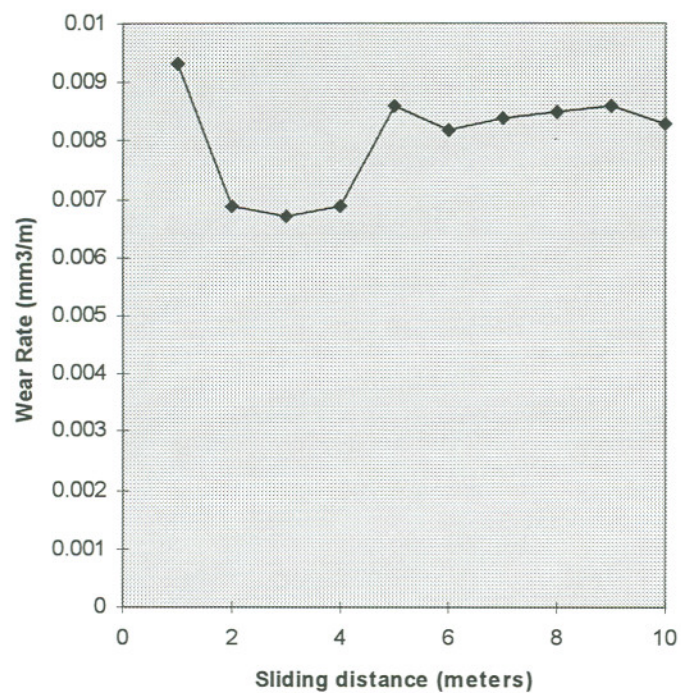


Figure 24
Wear Rate Vs Sliding Distance of
Zirconium 702 with an Oxidized Surface Treatment
in DI water at 85°C

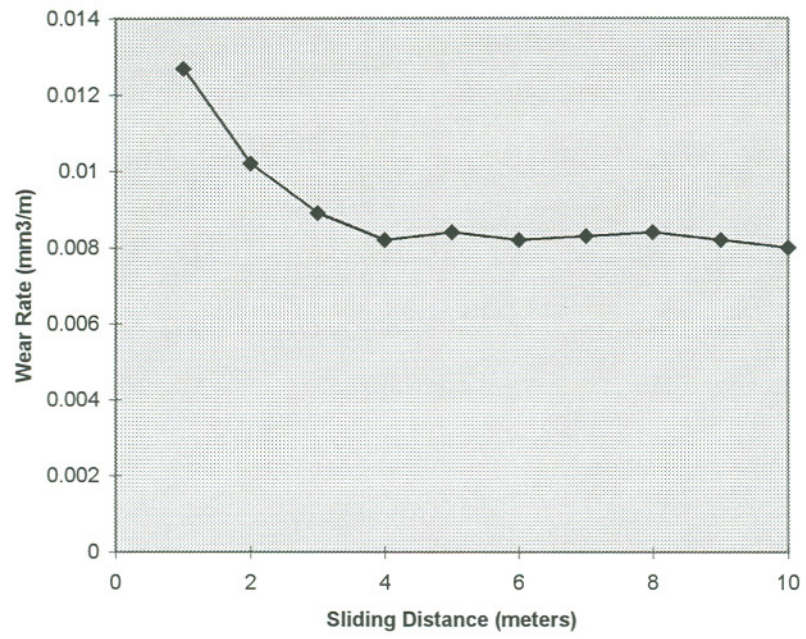


Figure 25
Wear Rate Vs Sliding Distance of
Stainless Steel 304L
in DI water at 85°C

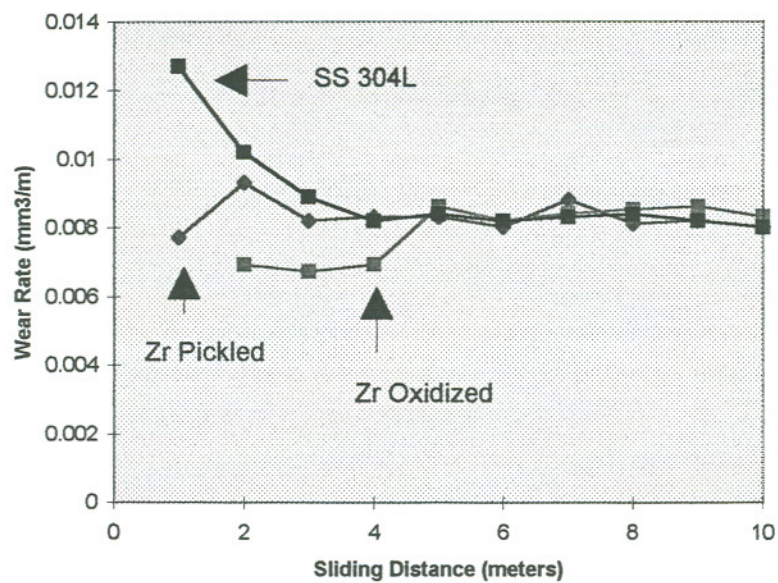


Figure 26
Comparison of Wear Rate Vs Sliding Distance of
Zirconium 702 with Pickled Surface Treatment,
Zirconium 702 with Oxidized Surface Treatment and
Stainless Steel 304L
in DI water at 85°C.

4.1.5 Corrosive Wear Experiments

Corrosive wear experiments were performed in green liquor at 85°C. Figures 27, 28 and 29 show volume loss for zirconium with a pickled surface treatment, zirconium with an oxidized surface treatment and for SS 304L, respectively. Figure 30 shows a direct comparison of the volume loss by all three specimens in the test conditions.

As with the experiments run in DI water, it was surprising that zirconium with a pickled surface treatment had an overall lower volume loss than the SS 304L specimen. As expected, Figure 30 shows that, of the three materials tested, zirconium with the oxidized surface treatment had the lowest volume loss. The missing data point at 3 meters for the oxidized specimen in Figure 28 was due to a loose specimen in the holder and that data point was discarded.

It is interesting to note that after the first approximately 4 meters of wear distance, the volume loss by the zirconium specimen with the oxidized surface treatment very nearly paralleled the volume loss by the zirconium specimen with a pickled surface treatment. This could be due to the weight-volume calculations and the slight density-volume difference between pure zirconium metal and zirconium metal overlaid with the thin oxide layer.

Figure 30 shows that the zirconium specimen with the oxidized surface treatment had the lowest volume loss of the three specimens tested. Figure 30 also shows that, unlike the wear experiments in DI water (Figure 20), the oxygen hardening below the visible oxide layer affected the volume loss only slightly throughout the 10 meter sliding distance. This is apparent by the linearity of the plot of volume loss vs. sliding distance and by the absence of a noticeable break in the slope after the visible oxide layer is removed.

In Figure 27, which shows the wear rate for zirconium with a pickled surface treatment in green liquor, the specimen exhibited an almost constant wear rate of approximately 0.002 mm³/m.

The wear rate for zirconium with the pickled surface, Figure 31, indicates an essentially constant wear rate over the test distance of 10 meters. Only a slight variation in the wear rate occurs at approximately 5 meters. At this point, the wear rate drops from $.02 \text{ mm}^3/\text{m}$ to approximately $.018 \text{ mm}^3/\text{m}$.

Figure 32 shows the wear rate for zirconium with an oxidized surface treatment. In this case, the wear rate does not level out until sometime after a sliding distance of 10 meters. The change in wear rate from the initial rate of $0.008 \text{ mm}^3/\text{m}$ to the final rate of $0.016 \text{ mm}^3/\text{m}$ is essentially linear. It appears that the wear rate for the specimen with the oxidized surface treatment will eventually reach the higher wear rate equal to rate for the pickled specimen. After reaching this point, at approximately $0.002 \text{ mm}^3/\text{m}$, the wear rate should follow closely the wear pattern of the pickled specimen. This seems reasonable, after the initial oxide layer and the oxygen strengthened sublayer is removed, the wear specimen should behave very similarly to the pickled specimen. At this point the only difference between the two specimens should be the very thin oxide layer and its associated oxygen strengthened sublayer which is still present on the walls of the oxidized specimen. Again, the missing data point was due to faulty mechanical connection and was discarded.

The SS 304L wear rate is shown in Figure 33. Although initially higher, the wear rate appears to level off at around 10 meters sliding distance to $0.025 \text{ mm}^3/\text{m}$.

Comparison of wear rate between the three specimens tested, Figure 34, indicates three unique wear patterns initially. Zirconium with a pickled surface treatment had an essentially uniform wear rate for the entire test distance. Zirconium with an oxidized surface treatment exhibited a wear rate which increased with distance. In contrast, the wear rate for the SS 304L specimen decreased over the test interval. In each case, however, it appears that the final steady state wear rate, attained over some distance, for each specimen will be essentially the same.

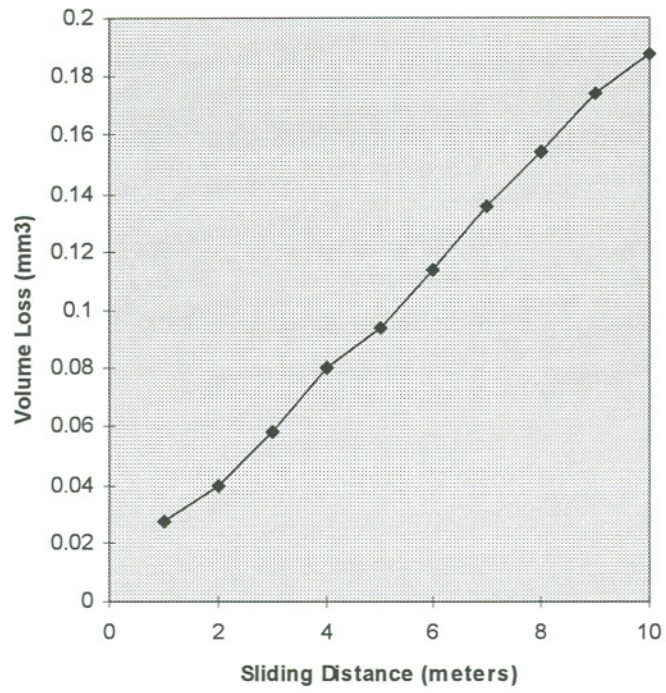


Figure 27
Volume Loss Vs Sliding Distance of
Zirconium 702 with Pickled Surface Treatment
in Green Liquor at 85°C

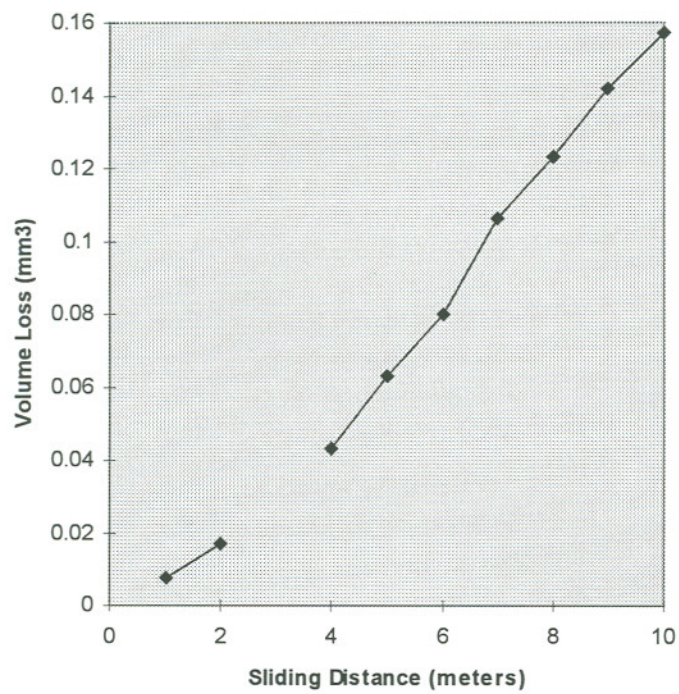


Figure 28
Volume Loss Vs Sliding Distance of
Zirconium 702 with Oxidized Surface Treatment
in Green Liquor at 85°C

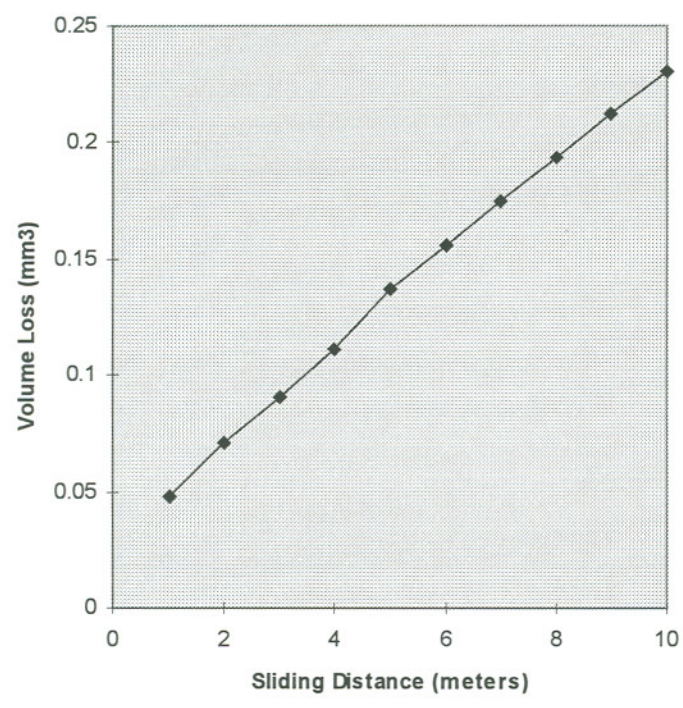


Figure 29
Volume Loss Vs Sliding Distance of
Stainless Steel 304L
in Green Liquor at 85°C

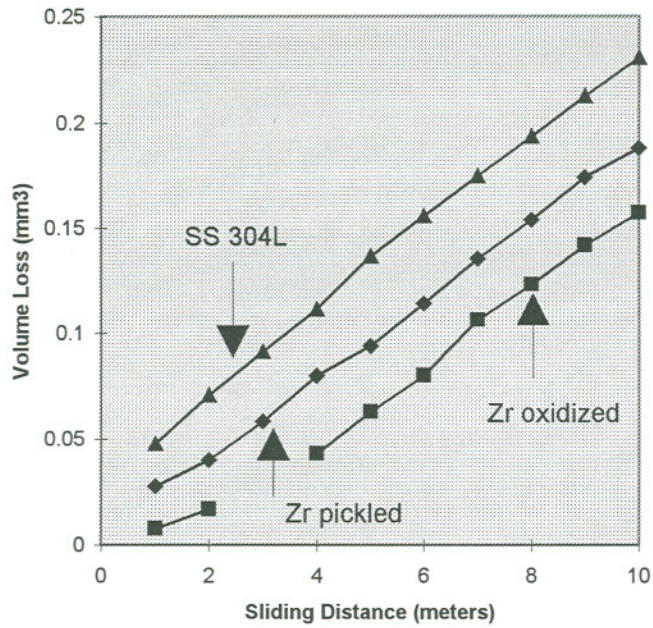


Figure 30
Comparison of Volume Loss Vs Sliding Distance of
Zirconium 702 with Pickled Surface Treatment,
Zirconium 702 with Oxidized Surface Treatment and
Stainless Steel 304L
in Green Liquor at 85°C

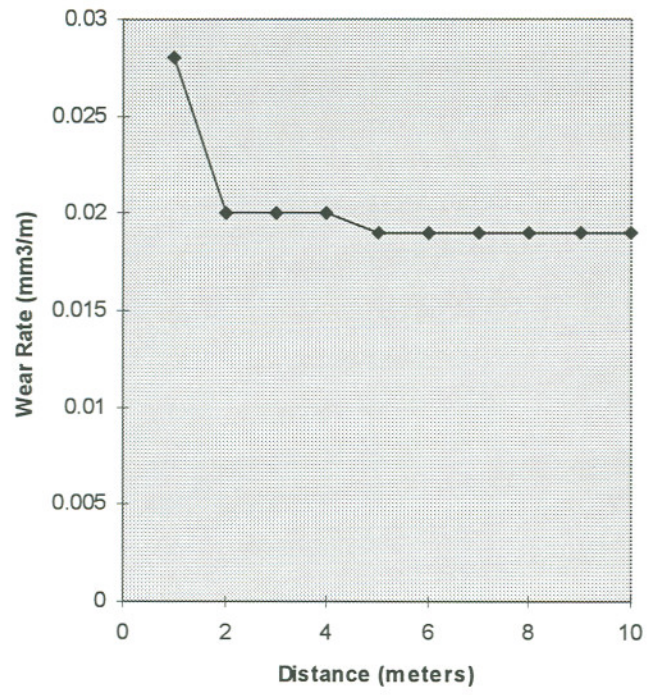


Figure 31
Wear Rate Vs Sliding Distance of
Zirconium 702 with Pickled Surface Treatment
in Green Liquor at 85°C

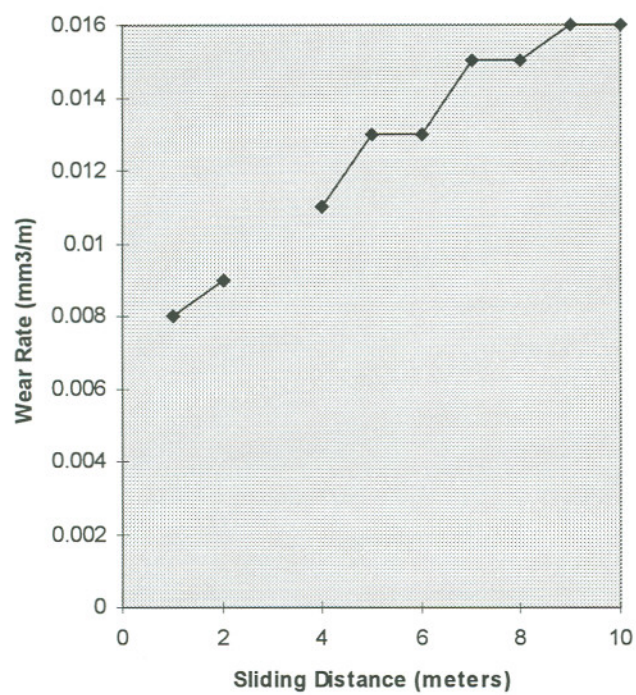


Figure 32
Wear Rate Vs Sliding Distance of
Zirconium 702 with Oxidized Surface Treatment
in Green Liquor at 85°C

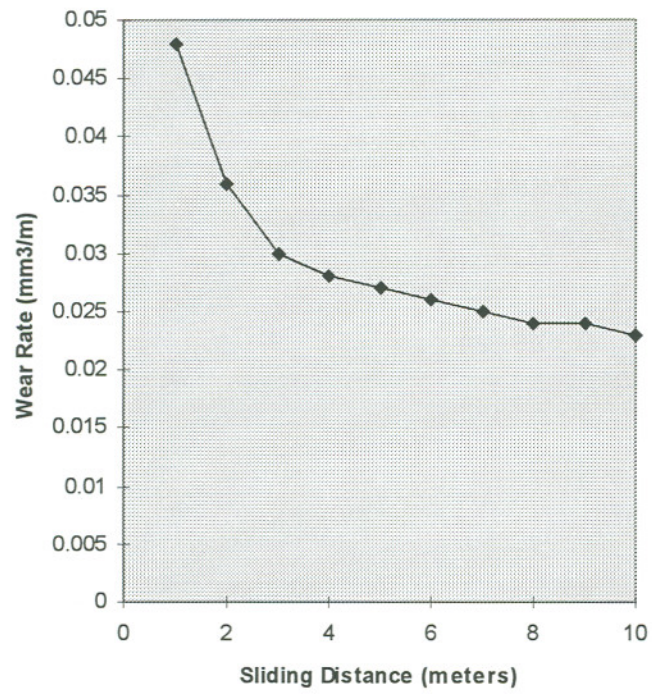


Figure 33
Wear Rate Vs Sliding Distance of
Stainless Steel 304L
in Green Liquor at 85°C

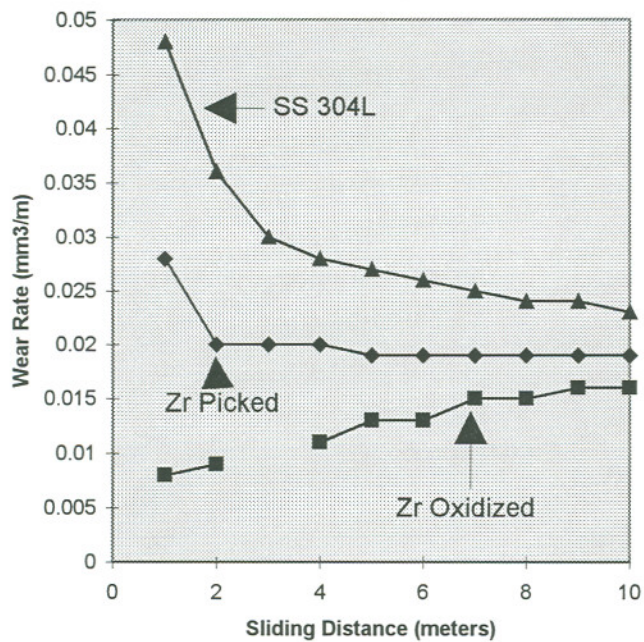


Figure 34
Comparison of Wear Rate Vs Sliding Distance of
Zirconium with Pickled Surface Treatment,
Zirconium with Oxidized Surface Treatment
and Stainless Steel 304L
in Green Liquor at 85°C

4.2 Determination of Corrosive Wear Synergism

The synergistic effect (S) between corrosion and corrosive wear can be calculated using the following equation.[2]

$$S = T - (W_o + C_o)$$

where

S - synergistic component when corrosion and wear act together

T - corrosive wear rate (when corrosion and wear act together)

W_o - wear rate in the absence of corrosion (pure wear only)

C_o - corrosion rate in the absence of wear (pure corrosion only)

Table 19 shows the experimental summary of values calculated for the materials under investigation.

The volume loss due to pure corrosion, as determined through Polarization Resistance measurements, is negligible. Because of this, the volume loss difference between the pure wear experiment, in DI water, and the corrosive wear experiment, in green liquor, is the synergism.

Table 19
Cumulative Volume Loss (mm³)

Material	T Corrosive Wear	C _o Corrosion Only	W _o Abrasion Only	Synergy T -(C _o + W _o)	% Synergy Synergy/T
Zr Pickled Surface	0.107	2.85 X 10 ⁻⁴	0.045	0.062	57.9
Zr Oxidized Surface					
1-5 meters	0.033	2.0 X 10 ⁻⁶	0.024	0.009	27.5
6-10 meters	0.122	----	0.067	0.055	44.9
SS 304L	0.143	1.4 X 10 ⁻⁴	0.046	0.097	67.7

The percent synergism calculation, as shown in Table 19, gives an indication of the interaction between corrosion and wear acting together. The higher the percent synergism, the greater this interaction. In the case of zirconium with the pickled surface treatment the synergism is 57.9%. This indicates that 57.9% of the total volume loss is due to the synergism between corrosion and wear.

For zirconium with the oxidized surface treatment, the synergism was lower at 27.5% for the first 5 meters. For the next 5 meters the synergism increased to 44.9%. As expected, the synergism effect for zirconium with the oxidized surface treatment is lower than for the zirconium with the pickled surface treatment. The zirconium with the pickled surface treatment had a synergism of 57.9%.

SS 304L exhibited the highest interaction between wear and corrosion with 67.7% synergism. This was unexpected considering that SS 304L is considerably harder than Zr 702.

Chapter 5 Conclusions

1. Based on open circuit potential measurements, zirconium with a pickled surface treatment and zirconium with an oxidized surface treatment showed less negative potentials when compared with SS 304L in green liquor at 85°C.
2. Polarization Resistance measurements indicated that zirconium with the oxidized surface treatment has the lowest corrosion rate of the three materials tested in green liquor at 85°C.
3. Wear experiments in both DI water at 85°C and green liquor at 85°C show that volume loss of the zirconium specimens with the oxidized surface treatment was low for the first 5 meters of sliding distance. Once this oxide layer was removed by abrasion, the volume loss of the oxidized specimens approached that of the zirconium with the pickled surface treatment.
4. Based on corrosive wear experiments, the zirconium with the oxidized surface treatment exhibits the lowest corrosive wear rate (T) of the three materials tested in green liquor at 85°C.
5. Synergy calculations showed lower interaction for both zirconium surface conditions in green liquor at 85°C as compared to SS 304L.

6. Synergy calculations also showed that in green liquor at 85°C zirconium with the oxidized surface treatment had the lowest interaction for the first 5 meters of sliding distance. After the first 5 meters of sliding distance, the interaction between wear and corrosive wear approached that of the zirconium with the pickled surface treatment.

Chapter 6

Future Work

1. The Kraft pulping process presents numerous opportunities for investigating the corrosion behavior as well as the wear behavior of reactive metals. The recausticizing circuit of a typical Kraft pulping plant has a wide variation in chemistries for the solutions being reconstituted. Wear testing could be performed on a wide variety of solutions and in a wide range of environments related to the pulping system.
2. Future work could include testing the wear performance of zirconium and its alloys in other pulping environments.
3. Identifying the difference in passive film morphology in the two passive regions identified by the potentiodynamic polarization scans of zirconium with a pickled surface treatment could help in understanding the nature of passive films, which are developed on the surface of zirconium.
4. Actual wear testing in a simulated agitator assembly, using solutions used in the Kraft process, could be performed to validate wear resistance of zirconium and its alloys under more realistic conditions.

Chapter 7 Bibliography

- [1] Angela Wensley and Patrick Champagne, "Effects of Sulfidity on the Corrosivity of White, Green, and Black Liquors", Paper No. 281, Corrosion/99, San Antonio, Texas, 1999. pp 1-10.
- [2] Fritz J. Friedersdorf and Gordon R. Holcomb, "Pin-on-disk Corrosion-Wear test", Journal of Testing and Evaluation, Vol. 26, No. 4, July 1998, pp 352-357.
- [3] ASTM G-119, "Standard Guide for Determining Synergism Between Wear and Corrosion", ASTM, Philadelphia, Pa, 1999.
- [4] S. Mischler, S. Debaud, and D. Landolt, "Wear-Accelerated Corrosion of Passive Metals in Tribocorrosion Systems", Journal of the Electrochemical Society, Vol. 145, No. 3, March 1998, pp. 750-758.
- [5] S.W. Watson, F.J.Friedersdorf, B.W.Madson, S.D.Cramer, "Methods of Measuring Wear-Corrosion Synergism", Presented at 10th International Conference on Wear of Materials, Boston, Ma., April 9-13, 1995, pp 476-484.
- [6] S. Zhou, M.M. Stack, and R.C. Newman, "Characterization of Synergistic Effects Between Erosion and Corrosion in an Aqueous Environment Using Electrochemical Techniques", Corrosion, Vol. 52, No. 12, 1996, pp 934-945.
- [7] Denny A Jones, Principles and Prevention of Corrosion, 2nd Edition, Prentice Hall Inc. Upper Saddle River, NJ, 1996.
- [8] John C. Haygarth and Lloyd J. Fenwick, "Improved Wear Resistance of Zirconium by Enhanced Oxide Films", Thin Solid Films, Paper No. 118, Presented at International Conference on Metallurgical Coating, San Diego, CA., April 9-13, 1984, pp 351-362.

- [9] M.B. Abuzriba, R.A. Dodd, F.J. Worzala, and J.R. Conrad, "Wear Corrosion: Separation of the Components of Corrosion and Wear", *Corrosion*, Vol. 48, No.1, 1992, Technical Note; pp 2-4.
- [10] Marcel Pourbaix, *Atlas of Electrochemical Equilibria in Aqueous Solutions*, Pergamon Press, New York, 1966, pp 223-229.
- [11] United States Department of Interior, *Mineral Industry Surveys, Zirconium and Hafnium: Annual Review*, United States Bureau of Mines, Reston Va., 1998.
- [12] Carol J. Cort, and William L. Bohn, "Alkaline Peroxide Mechanical Pulping of Hardwoods", *TAPPI Journal*, Vol.74, No. 6, June, 1991, pp 79-84.
- [13] Martin Zimmermann, Rudolf Patt, and Othar Kordsachia, W. Densmore Hunter, "ASAM Pulping of Douglas-fir followed by a chlorine-free bleaching sequence", *TAPPI Journal*, Vol. 74, No. 11, Nov 1991, pp 129-134.
- [14] Koki Fujita, Ryuichiro Kondo and Kokki Sakaii, Yoshinori Kashino, Tomoaki Nishida, and Yoshimasa Takahara, "Bioleaching of Kraft Pulp using White-rot Fungus IZU-154", *TAPPI Journal*, Vol. 74, No. 11, Nov 1991, p 123.
- [15] Te-Lin Yau, "The performance of Zirconium Alloys in Sulfide Environments", Paper 129, *Corrosion/82*, Houston, Texas, 1982, pp 1-14.
- [16] W.J. Schumacher, "Corrosive Wear Principles", Paper No. 316, *Corrosion/93*, New Orleans, Louisiana, 1993, pp 50-53.
- [17] George T. Austin, *Shreves Chemical Process Industries*, 5th Edition, McGraw-Hill Inc, New York, 1984, pp 613-627.
- [18] ASTM G-2, "Aqueous Corrosion Testing of Samples of Zirconium and Zirconium Zirconium Alloys", ASTM, Philadelphia, Pa, 1999.
- [19] ASTM G-5, "Standard Reference Method for Making Potentiostatic and Potentiodynamic Anodic Polarization Measurements", ASTM, Philadelphia, Pa, 1999.
- [20] John C. Haygarth, "Zirconium in a salt bath", *Outlook*, Teledyne Wah Chang Albany, Vol. 6, No.1, 1985, pp 2.
- [21] Te-Lin Yau, "Zirconium for the Changing Pulp and Paper Industry", Paper No. 436, *Corrosion/93*, New Orleans, Louisiana, 1993, pp 1-10.

- [22] Encyclopedia of Chemical Technology, Vol. 18, 4th Edition. John Wiley & Sons Inc, New York, NY, 1996, pp 1-3.
- [23] Robert H. Wehrenberg II, Senior Editor, "Oxidized Zirconium", Mechanical Engineering, Vol. 98, July 1983, pp 46-49.
- [24] ASTM G-40, "Standard Terminology relating to Erosion and Wear", ASTM, Philadelphia, Pa, 1997.
- [25] R.A. Yeske, "Corrosion by Kraft Pulping Liquors", Metals Handbook 9th Edition, Vol 13, American Society for Metals, 1987, pp 1208-1214.
- [26] Te-Lin Yau, "Highly Corrosion Resistant Metals for the Pulp and Paper Industry", 1990 TAPPI Engineering Conference, Atlanta, Ga.(1990): TAPPI Journal, Vol. 74, No. 3, 1991, pp. 149.
- [27] Te-Lin Yau, "Preoxidizing Zr for Corrosion Control", Outlook, Teledyne Wah Chang Albany, Vol.17, No. 2, 1996, p 5.
- [28] Willard E. Kemp, "Nobleizing: Creating Tough, Wear resistant surfaces on Zirconium", Outlook, Teledyne Wah Chang Albany, Vol. 11, No. 2, pp 4-5, 1990.
- [29] Philip A. Schweitzer, Corrosion Engineering Handbook, Marcel Dekker, Inc, New York, NY, 1996. pp 195-252.
- [30] Materials Technology Institute of the Chemical Process Industries, Inc., "Technology Roadmap for Materials of Construction, Operation and Maintenance in the Chemical Process Industries", Dec 1998. Available:[http:// www.mti-link.ore/members/documents/techroadmap.pdf](http://www.mti-link.ore/members/documents/techroadmap.pdf). [Viewed: September 20, 2000].
- [31] T.L. Yau, J. Fahey, and D.R. Holmes, "Performance of Zirconium in bleaching solutions", Proceedings of 1993 TAPPI Engineering Conference, Orlando, Florida, September 20-23, 1993, pp 1013-1020.
- [32] Fahey, Holmes, and T.L. Yau, "Control and Monitoring of the Localized Corrosion of Zirconium in Acidic Chloride Solutions", Corrosion/95, Paper No. 246, Orlando, Florida, 1995. Pp 1-14.
- [33] Alan M. Bateman, Economic Mineral Deposits, 2nd Edition, John Wiley & Sons, Inc., New York, NY., 1959, pp 626.
- [34] W.J. Schumacher, "Metals for Nonlubricated Wear", Machine Design, Vol. 48, No. 6, March 11, 1976, p 57.

- [35] Lange's Handbook of Chemistry, 13th Edition, McGraw-Hill Book Company, New York, NY, 1985.
- [36] Te-Lin Yau, "Performance of Zirconium and Zirconium Alloys in Organics", Journal of Testing and Evaluation, Vol. 24, No. 2, March 1996, pp 110-118.
- [37] F. Albert Cotton and Geoffrey Wilkinson, Advanced Inorganic Chemistry, 3rd Edition, Interscience Publishers, New York, NY, 1972, pp 927-933.
- [38] Bruce D. Craig, and David S. Anderson, Handbook of Corrosion, 2nd Edition, ASM International, Materials Park, Oh., 1995, pp 62-66.
- [39] Te-Lin Yau, "Zircadyne Improves Organic Production", Outlook, Teledyne Wah Chang Albany, Vol. 16, No.1, pp 1-11, 1995.
- [40] Eugene Ryshkewitch, Oxide Ceramics, Physical Chemistry and Technology, Academic Press, New York, 1960, pp 381.
- [41] Herbert H. Uhlig, R. Winston Revie, Corrosion and Corrosion Control, 3rd Edition, John Wiley & Sons, New York, 1985.

Biographical Sketch

Derrill Holmes was born March 30, 1948 in Albany, Oregon. He received a B.S. in Geology from Oregon State University in 1976. In 1976 he worked in southwestern Oregon as an exploration geologist and in Montana where he managed a small commercial mining operation. Since 1977 he has worked at Wah Chang in Albany, Oregon. The last 20 years have been in the corrosion laboratory of the technical services group. He has attended Oregon Graduate Institute of Science & Technology in the Materials Science Department since 1997.